



# Long-Profile Evolution of Transport-Limited Gravel-Bed Rivers

Andrew D. Wickert<sup>1</sup> and Taylor F. Schildgen<sup>2,3</sup>

<sup>1</sup>Department of Earth Sciences and Saint Anthony Falls Laboratory, University of Minnesota, Minneapolis, Minnesota, USA.

<sup>2</sup>Institut für Erd- und Umweltwissenschaften, Universität Potsdam, 14476 Potsdam, Germany.

<sup>3</sup>Helmholtz Zentrum Potsdam, GeoForschungsZentrum (GFZ) Potsdam, 14473 Potsdam, Germany.

*Correspondence to:* A. D. Wickert (awickert@umn.edu)

**Abstract.** Alluvial and transport-limited bedrock rivers constitute the majority of fluvial systems on Earth. Their long profiles hold clues to their present state and past evolution. We currently possess first-principles-based governing equations for flow, sediment transport, and channel morphodynamics in these systems, which we lack for detachment-limited bedrock rivers. Here we formally couple these equations for transport-limited gravel-bed river long-profile evolution. The result is a new predictive relationship whose functional form and parameters are grounded in theory and defined through experimental data. From this, we produce a power-law analytical solution and a finite-difference numerical solution to long-profile evolution. Steady-state channel concavity and steepness are diagnostic of external drivers: concavity decreases with increasing uplift, and steepness increases with increasing sediment-to-water supply ratio. Constraining free parameters explains common observations of river form: To match observed channel concavities, gravel-sized sediments must weather and fine – typically rapidly – and valleys must widen gradually. To match the empirical square-root width–discharge scaling in equilibrium-width gravel-bed rivers, downstream fining must occur. The ability to assign a cause to such observations is the direct result of a deductive approach to developing equations for landscape evolution.

## 1 Introduction

Mountain and upland streams worldwide move clasts of gravel (>2 mm). In so doing, they consistently reshape their beds and – unless they are fully bedrock-confined – their bars and banks as well (Parker, 1978; Brasington et al., 2000, 2003; Church, 2006; Eke et al., 2014; Phillips and Jerolmack, 2016; Pfeiffer et al., 2017). Such rivers are responsible for carrying gravel out of the mountains, and hence maintaining their topographic relief. They also can transport sediment across moderate-relief continental surfaces and into sedimentary basins.

Geomorphologists commonly separate rivers into two broad categories based on the factor that limits their ability to change their long profile: detachment-limited and transport-limited (Whipple and Tucker, 2002). Detachment-limited rivers incise at a rate that is set by the mechanics of river incision into bedrock. Transport-limited rivers can incise or aggrade at a rate that is set by the divergence of sediment discharge through a river or valley cross-section.

Here we present a new derivation for transport-limited gravel-bed river long-profile evolution that is based on relationships derived from theory, field work, and experimentation. We argue that developing this deductive approach – considering specific process relationships – is essential to advancing fluvial geomorphology and landscape evolution.



Much past work has focused on an inductive “stream-power” based formulation for detachment-limited river incision, in which erosion rate is proportional to drainage area (as a proxy for geomorphically-effective discharge) and channel slope (e.g., Gilbert, 1877; Howard, 1980; Howard and Kerby, 1983; Whipple and Tucker, 1999; Gasparini and Brandon, 2011; Harel et al., 2016). This rule is intuitive, and may also be described in terms of the rate of power dissipation against the river bed.

5 However, such a generalized approach is agnostic to geomorphic processes. Efforts to understand the detailed mechanics of abrasion (Sklar and Dietrich, 1998, 2004; Johnson and Whipple, 2007) and quarrying (Dubinski and Wohl, 2013), the two main mechanisms of bedrock river erosion (Whipple et al., 2000), have aided efforts to generate mechanistic models for bedrock incision (Gasparini et al., 2006; Chatanantavet and Parker, 2009). However, the large number of measured parameters required for these relationships limits their use in practice and/or requires simplifications, such that the basic stream-power law remains

10 the dominant model for detachment-limited rivers.

Writing a set of equations to describe the long-profile evolution of transport-limited gravel-bed rivers, on the other hand is aided by an extensive history of study that can be directly applied to models of long-profile evolution. This includes open-channel flow and flow resistance that can be applied to sediment-covered channels (e.g., Nikuradse, 1933; Keulegan, 1938; Limerinos, 1970; Aguirre-Pe and Fuentes, 1990; Parker, 1991; Clifford et al., 1992), bed-load transport (e.g., Shields, 1936;

15 Meyer-Peter and Müller, 1948; Gomez and Church, 1989; Parker et al., 1998; Wilcock and Crowe, 2003; Wong and Parker, 2006; Bradley and Tucker, 2012; Furbish et al., 2012), and fluvial morphodynamics (e.g., Lane, 1953; Leopold and Maddock, 1953; Parker, 1978; Ikeda et al., 1988; Ashmore, 1991; Church, 2006; Pitlick et al., 2008; Eke et al., 2014; Bolla Pittaluga et al., 2014; Blom et al., 2016; Phillips and Jerolmack, 2016; Pfeiffer et al., 2017; Blom et al., 2017). Critical to the present work is the fact that the authors of these past studies have developed theory, tested it in both laboratory and field settings, and

20 empirically determined the values of the relevant coefficients (e.g., Wong and Parker, 2006). Furthermore, bedrock channels can act as transport-limited systems (Johnson et al., 2009), meaning that an approach to transport-limited conditions may be able to describe the evolution of not only alluvial rivers, but rivers across much of Earth’s upland surface. Based on this past research, we are able to write a simple and consistent set of equations for transport-limited gravel-bed river long-profile evolution that eschews tunable parameters, common in stream-power approaches to river long-profile evolution (Howard and

25 Kerby, 1983; Whipple and Tucker, 1999, 2002) for those based on experimentation, measurements, and theory.

Here we link sediment transport and river morphodynamics to develop equations to describe gravel-bed river long profiles and, as a necessary extension, their tightly-coupled width evolution. Our approach, which allows channel widths to self-form, modifies channel roughness as a function of flow depth and grain size, and allows for changes in sediment supply and base level, is complementary to a recent set of relations for alluvial river long profile shapes developed by Blom et al. (2016) and

30 Blom et al. (2017), who explore equilibrium alluvial river long profile shapes in response to changes in grain size, slope, and width. Our approach and discussion are tailored to time-scales from decades to millions of years, a broad range that results from the direct derivation of these equations and their parameter values from fundamental physics, observations, and laboratory experiments.

Our approach is outlined as follows: First, we generate fully-coupled equations of gravel transport and fluvial morphodynamics to describe how channel long profiles change. Second, we investigate how the governing equations for gravel-bed rivers

35



differ when we assume a channel with a self-formed equilibrium width versus when their width is externally set. Third, we derive both analytical and numerical solutions for the case of an equilibrium-width channel, which is nearly ubiquitous in nature (Phillips and Jerolmack, 2016). Fourth, we quantify the constants for stream-power-based bed-load transport from Whipple and Tucker (2002) in a dimensionally-consistent form that is based on our derived equations and the sizes of storm footprints. Fifth, we demonstrate that most gravel clasts in the landscape must be removed rapidly by weathering and/or downstream fining in order to produce rivers with concavities that lie within observed ranges. Sixth, we show that valley widening is required to produce rivers with observed concavities. Seventh, we investigate both steady-state and transient effects of base-level change (e.g., through tectonics) and sediment-to-water discharge ratio (via climate and/or tectonics) on river long profiles, and demonstrate that the former changes concavity while the latter changes steepness. Eighth and finally, we derive that downstream fining and channel concavity must combine to be the mechanistic cause of channel width scaling with the square root of water discharge ( $b \propto Q^{0.5}$ ) (Lacey, 1930; Leopold and Maddock, 1953), at least in equilibrium-width (including near-threshold) transport-limited gravel-bed rivers.

## 2 Derivations

We consider gravel-bed rivers to exist in one of two states: equilibrium-width and fixed-width. In the first, we assume that the channel-forming (i.e. bankfull) shear stress on the bed remains a constant ratio of the critical shear stress that sets the threshold for initiation of sediment motion (after Parker, 1978). The channel width is set to maintain this ratio. In the second, the channel and valley width are assumed to be identical in order to use the one-dimensional form of the sediment continuity equation, called the Exner equation (e.g., Paola et al., 1992; Whipple and Tucker, 2002; Blom et al., 2016). A third and more general case exists in which one externally imposes both channel and valley width. We do not address this case here, though it may be solved using the provided equations.

Our primary focus here is on equilibrium-width rivers, which are common throughout the world (Phillips and Jerolmack, 2016; Pfeiffer et al., 2017). Most maintain a bed shear stress that is slightly greater than that for the initiation of motion (Parker, 1978; Phillips and Jerolmack, 2016), and this near-threshold condition is characteristic of both fully alluvial and alluvial-mantled bedrock streams (Phillips and Jerolmack, 2016). Rivers in rapidly-uplifting mountain belts maintain a bed shear stress that can be much greater than that for initiation of particle motion; this results in higher sediment discharges that help to balance the high inputs of sediment that result from rock uplift (Pfeiffer et al., 2017). Although these rivers do not exist in a near-threshold state, they maintain an equilibrium width corresponding to their ratio of bed shear stress to critical shear stress for initiation of motion that allows them to transport the sediment that they are supplied (Pfeiffer et al., 2017).

We split our derivations into sections on equilibrium-width (Section 2.1) and fixed-width (Section 2.2) rivers. We first develop a sediment discharge relationship as a function of channel morphology. This portion of the derivation can apply to both alluvial (transport-limited) and bedrock (both transport- and detachment-limited) rivers. Simulating detachment-limited rivers in which abrasion is the dominant mechanism of river incision requires sediment-flux-dependent erosion relationships (Sklar and Dietrich, 2001; Whipple and Tucker, 2002; Sklar and Dietrich, 2004; Gasparini et al., 2006, 2007), which we do not

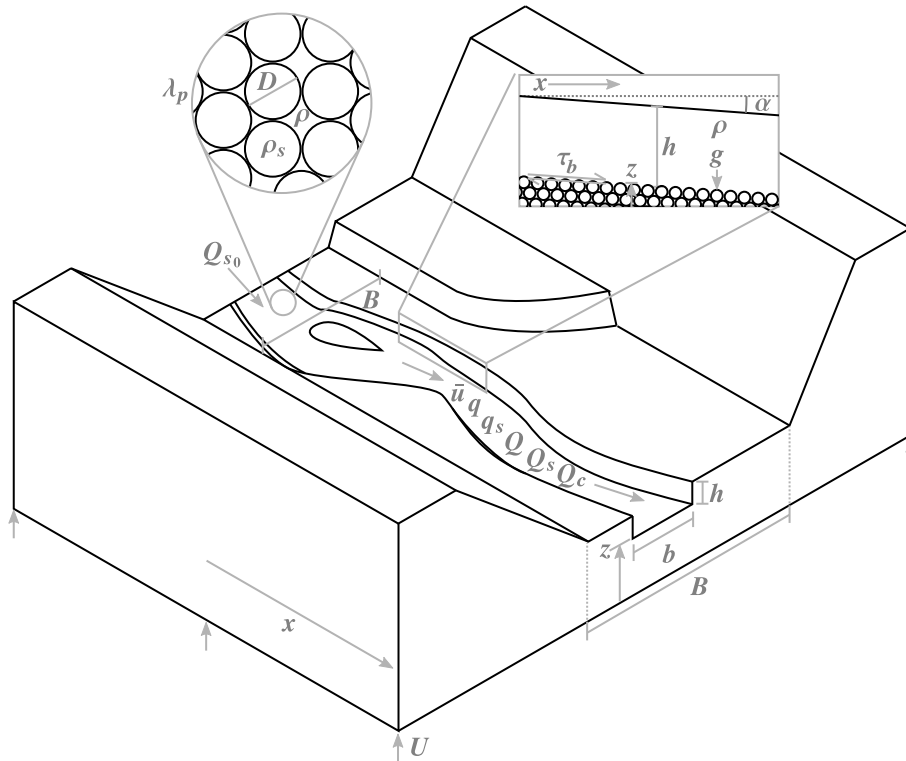


**Figure 1.** Schematic block diagram of sediment transport through a reach of a transport-limited river. Variables are defined in the text and in the “Notation” list at the end of the paper. The balance of sediment input, sediment output, and uplift determine whether the river bed at each point downstream will rise, fall, or remain at a constant elevation.

discuss in detail here. We focus on alluvial and transport-limited bedrock cases by applying a statement of sediment volume balance (the Exner equation) to develop a differential equation that describes alluvial river long-profile evolution over time. The width closure for the equilibrium-width gravel-bed river produces a mathematically clean solution from which intuition can be readily gained, and this is the focus of our discussion. The fixed-width case, which is characteristic of an engineered  
 5 gravel-bed river with rigid walls, is included for contrast with the equilibrium-width case and comparison with studies in which an externally-set width is assumed (e.g., Blom et al., 2016, 2017).

## 2.1 Equilibrium-width river

We derive an equation for the evolution of the long profile of an equilibrium-width gravel-bed river that lies within a valley whose shape is arbitrary (though at least as wide as the channel) and may evolve through time. We first state the Exner equation  
 10 for conservation of bed-load sediment discharge ( $Q_s$ ) for a river with sinuosity (river length divided by valley length)  $S$  in a



valley of width  $B$  (Figure 1):

$$\frac{\partial z}{\partial t} = -\frac{S}{1 - \lambda_p} \left( \frac{1}{B} \frac{\partial Q_s}{\partial x} - \frac{Q_s}{B^2} \frac{\partial B}{\partial x} \right) \quad (1)$$

Here,  $z$  is the elevation of the river bed surface, and is often also denoted as  $\eta$  in the alluvial river literature. Time is represented by  $t$ .  $\lambda_p$  is porosity, for which 0.65 is a representative value (consistent with Beard and Weyl, 1973), and  $x$  is distance down-  
 5 stream.  $B$  is the width of the river valley at the current level of the river bed; it may change with changes in river bed elevation and/or as the valley widens or narrows over time. These terms scale the result: a higher porosity means that less sediment must be eroded or deposited to produce the same change in bed elevation (i.e. aggradation or incision). A wider valley means that more sediment must be moved to produce a given amount of aggradation or incision. As channel sinuosity increases, a longer  
 10 length of channel traverses each valley cross-section, thus reducing the fraction of the valley width,  $B$ , that each channel cross section must fill or empty in order to cause the long profile to aggrade or incise. Here we approximate sinuosity as a term that may be averaged over length-scales and time-scales that correspond to channel migration and valley filling or incision, such that we treat it as a constant that may change only gradually in space.

Following this definition of a continuity equation, we take several steps towards developing a simple formulation for the total discharge of sediment through the river,  $Q_s$ . Once we find the correct expression for this value, we insert it into Equation  
 15 1, which we then simplify into a final differential equation for transport-limited gravel-bed river long-profile evolution.

Towards this eventual goal, our second step is to define bed-load sediment discharge per unit width,  $q_s$ , where

$$q_s = \frac{Q_s}{b} \quad (2)$$

Here,  $b$  is the width (breadth) of the river channel ( $b \leq B$ ). We compute bed-load transport using the Wong and Parker (2006) formulation of the Meyer-Peter and Müller (1948) formula. This formula is semi-empirical: its core form is based on a balance  
 20 of shear stress along the bed driving particle motion and particle weight resisting that motion, but its power-law functional form as well as its coefficients and exponents are fit to the results of laboratory experiments. More fully theory-based formulations are under development (Furbish et al., 2012; Fathel et al., 2015) and promise significant advances in our understanding and prediction of sediment transport. Our choice to use the Meyer-Peter and Müller (1948) formulation stems from its longevity, its simplicity, the fact that it has been well tested (Wong and Parker, 2006), and its compatibility with the channel-width closure  
 25 resulting from the work of Parker (1978). We stress that our general set of steps to deriving equations for long-profile evolution may be repeated for any sediment transport relation.

$$q_s = \begin{cases} 0 & \text{if } |\tau_b^*| \leq \tau_c^* \\ -\text{sgn}\left(\frac{dz}{dx}\right) \phi \left(\frac{\rho_s - \rho}{\rho}\right)^{1/2} g^{1/2} (|\tau_b^*| - \tau_c^*)^{3/2} D^{3/2} & \text{if } |\tau_b^*| > \tau_c^* \end{cases} \quad (3)$$

Here,  $\text{sgn}$  is the signum function (Equation 4),  $\phi = 3.97$  (Wong and Parker, 2006) is an experimentally-derived sediment transport rate coefficient.  $\rho_s$  is sediment density,  $\rho$  is water density, and  $g$  is acceleration due to gravity.  $|\tau_b^*|$  is the magnitude  
 30 of the dimensionless basal shear stress (defined in Equation 7, below), and is also called the “Shields stress” (after Shields, 1936).  $\tau_c^* = 0.0495$  (Wong and Parker, 2006) is the experimentally-derived dimensionless critical shear stress for initiation of



particle motion, and is also called the “critical Shields stress”.  $D$  is a representative sediment grain (particle) size, which we take to be the median gravel clast diameter. The signum function,  $\text{sgn}$ , is defined as:

$$\text{sgn}([\text{value}]) = \begin{cases} -1 & \text{if } [\text{value}] < 0, \\ 0 & \text{if } [\text{value}] = 0, \\ 1 & \text{if } [\text{value}] > 0. \end{cases} \quad (4)$$

The explicit signum and  $dz/dx$  terms are included in the place of the commonly-used “slope” term to (1) relax the assumption that the downslope direction is known, (2) allow the numerical model to self-consistently handle changes in flow direction, and (3) enable the sign and the magnitude of the slope to be separated in equations that include a slope term raised to a power, which prevents a spurious imaginary part of the solution.

While the Meyer-Peter and Müller (1948) equation is strictly valid only for a single grain size class, it is often an acceptable approximation for natural rivers with multiple size classes (Gomez and Church, 1989; Paola and Mohrig, 1996). Interactions among multiple grain size classes may cause a condition of “equal mobility” in gravel-bed rivers (e.g., Parker et al., 1982): small grains become trapped inside pits between larger grains, while large grains rest on a carpet of smaller grains and thus are exposed to more of the force of the flow. Even where significant deviations from equal mobility are observed,  $\tau_c^*$  for the 50<sup>th</sup> percentile grain size ( $D_{50}$ ) remains constant (Komar, 1987; Komar and Shih, 1992). For the representative grain size ( $D$ ) in Eq. 3 (and Eq. 28, below), Wong and Parker (2006) used the mean size of uniform gravel. We suggest the median grain size ( $D_{50}$ ) as representative of  $D$  for the mixed-size sediment of natural rivers due to its relative ease of standardized measurement (Wolman, 1954) and constant dimensionless critical shear stress for the initiation of motion (Komar, 1987; Komar and Shih, 1992; Paola and Mohrig, 1996). Regardless of this choice,  $D$  cancels out in our formulation for equilibrium-width gravel-bed rivers, starting in Equation 19.

Basal shear stress induces a drag force on the grains and drives sediment transport. To compute this basal shear stress ( $\tau_b$ ), we invoke the normal flow (steady, uniform) assumption, the wide-channel approximation ( $b \gg h$ , where  $h$  is the flow depth), and the small-angle formula (Figure 1, upper right inset):

$$\begin{aligned} \tau_b &= -\rho gh \sin \alpha \\ &\approx -\rho gh \frac{dz}{dx} \end{aligned} \quad (5)$$

Here,  $\tau_b$  is defined to be positive in the downslope direction (i.e. positive in the direction of positively-directed sediment transport) and  $\alpha$  is the angle between the plane of the water surface and the horizontal. The water surface and bed surface slopes are assumed to be parallel (following the normal flow assumption). In order to self-consistently represent the direction of sediment transport when  $\tau_b$  is raised to a power, we separate the magnitude (absolute value) of shear stress from its direction (signum function) by following a similar approach to that taken for Equation 3. Following the geomorphic convention of writing the magnitude of slope as  $S = |dz/dx|$ , we can write:

$$|\tau_b| = \rho gh S \quad (6)$$



The drag force on sediment grains induced by basal shear stress is resisted by the submerged weight of the grains. The ratio of these forces defines the Shields stress.

$$\tau_b^* = \frac{\tau_b D^2}{(\rho_s - \rho)gD^3} = \frac{\tau_b}{(\rho_s - \rho)gD} \quad (7)$$

In gravel-bed rivers, all of the shear stress is assumed to act as skin friction, meaning that it is directly imparted to the particles instead of being partially absorbed as form drag on larger-scale features (e.g., bedforms). When this dimensionless stress is in excess of the critical Shields stress ( $\tau_c^*$ ), particles begin to move.

In equilibrium-width gravel-bed rivers, the dimensionless basal shear stress at the channel-forming discharge is assumed to be maintained as a constant multiple of the dimensionless critical shear stress for initiation of sediment motion (Parker, 1978). This proportionality may be equally represented by dimensional stresses; we use the dimensionless Shields stresses here for consistency.

$$\tau_b^* = (1 + \epsilon)\tau_c^* \quad (8)$$

Parker (1978) derived based on theory and channel geometry that  $\epsilon \approx 0.2$  for self-formed gravel-bed rivers with mobile banks made of the same size gravel as the bed. This value has been found empirically and near-universally in rivers around the world outside of rapidly tectonically-uplifting environments (Phillips and Jerolmack, 2016; Pfeiffer et al., 2017).  $(1 + \epsilon)\tau_c^*$  is the dimensionless shear stress experienced by the bed of the channel when the shear stress experienced by the banks is equal to  $\tau_c^*$ . The Parker (1978) near-threshold gravel-bed river solution states that any excess stress would cause the banks to erode and the channel to widen, reducing the flow depth, and thereby decreasing  $\tau_b^*$  to  $(1 + \epsilon)\tau_c^*$ .

The channel-forming discharge, also termed the geomorphically-effective discharge, is equivalent to the bankfull flow in a self-formed gravel-bed river with gravel bars and banks. Blom et al. (2017) derived a method to differentiate the channel-forming discharge, defined as that required to maintain the channel slope, from the most effective discharges to move different grain size classes of sediments. This is a significant distinction, but one that will not be necessary for our modeling approach, as we consider only the discharges that are large enough to cause non-negligible geomorphic change. In a self-formed gravel-bed river, a near-threshold state is maintained in which  $\tau_b^* = 1.2\tau_c^*$  (Parker, 1978). We use this ratio between applied and critical shear stress to compute the numerical values for constants given in this derivation.

Substituting  $\tau_b^*$  in Equation 3 with its value given in Equation 8 reduces the complexity of Equation 3 by converting its excess shear stress terms ( $\tau_b^* - \tau_c^*$ ) into a constant (by a factor of  $\epsilon$ ) and requiring that only the case with a positive nonzero  $q_s$  be a plausible solution.

$$\begin{aligned} q_s &= \phi \left( \frac{\rho_s - \rho}{\rho} \right)^{1/2} g^{1/2} \epsilon^{3/2} \tau_c^{*3/2} D^{3/2} \\ &= k_{q_s} D^{3/2} \end{aligned} \quad (9)$$

In an equilibrium-width gravel-bed river,  $q_s$  is a function only of grain size. The value of  $k_{q_s} = 0.0157$  is obtained from  $\phi = 3.97$  (Wong and Parker, 2006),  $\rho_s = 2650 \text{ kg m}^{-3}$  (density of quartz),  $\rho = 1000 \text{ kg m}^{-3}$  (density of water),  $g = 9.807 \text{ m s}^{-2}$ ,  $\epsilon = 0.2$  (for a threshold-width channel Parker, 1978), and  $\tau_c^* = 0.0495$  (Wong and Parker, 2006).



It may be counterintuitive that sediment discharge per unit width increases with grain size. This is a result of the equilibrium-width argument. Channel geometry adjusts to maintain a constant excess basal shear stress regardless of grain size. However, larger grains have a greater vertical dimension: many small grains rolling or sliding along the bed will displace less mass than a single larger grain.

5 Equation 9 is physically valid only where  $b > D$  (see Equation 17, below) and is a good approximation only where  $b \gg h$  and  $h > D$  (see Equation 10, below). It seems likely that, at a flow width that is some small multiple of  $D$ , an equilibrium-width gravel-bed channel would be replaced by a boulder cascade or similar system that is more dispersed. While we do not investigate the exact point of this process-domain boundary, this forms a practical limit to the theory presented here.

For a self-formed gravel-bed channel, channel depth must satisfy Equation 8. Using the normal flow assumption, the depth–  
10 slope product (Equation 6) defines basal shear stress. Inserting the basal shear stress into Equation 8 and rearranging to solve for  $h$  results in:

$$h = \frac{\rho_s - \rho}{\rho} (1 + \epsilon) \tau_c^* \frac{D}{S} \quad (10)$$

Next, we compute mean water flow velocity ( $\bar{u}$ ) for a geomorphically-effective flow. We solve for mean flow velocity using the empirically-derived Manning–Strickler formulation (after Parker, 1991) of the Chézy equation. We first write the Chézy  
15 equation for steady, uniform flow,

$$\bar{u} = -\text{sgn}(\alpha) C_z \sqrt{ghS}. \quad (11)$$

Here,  $C_z$  is a factor that relates flow velocity to shear velocity, and  $\sqrt{ghS}$  is the shear velocity for steady, uniform flow. We then define  $C_z$ , following the Manning–Strickler formulation, as

$$C_z = 8.1 \left( \frac{h}{\lambda_r} \right)^{1/6} \quad (12)$$

20 The coefficient of 8.1 is empirical (Parker, 1991).  $\lambda_r$  is the characteristic roughness length scale; this is often denoted as  $k_s$ , but we reserve this notation for the channel steepness index in slope–area space (Section 5.2). The flow depth ( $h$ ) in the numerator and the roughness ( $\lambda_r$ ) in the denominator indicate that flow velocity increases as more flow is far from the boundary, and decreases with increasing boundary roughness. The gravel clasts themselves are the major source of roughness (and therefore flow resistance) in a gravel-bed river. Clifford et al. (1992) related grain size to roughness length to obtain the approximation  
25 that  $\lambda_r \approx 6.8D$ , where  $D$  is the median gravel clast diameter. Carrying this forward, but using a standard “equals” sign, produces an expression for flow velocity that depends only on constants and basic geomorphic parameters.

$$\bar{u} = -\text{sgn}(\alpha) 5.9g^{1/2} \frac{h^{2/3} S^{1/2}}{D^{1/6}} \quad (13)$$

The power-law form of the empirically-developed Manning–Strickler formulation closely approximates the more theoretical logarithmic boundary layer approach of Keulegan (1938) for ratios of depth to roughness length that are characteristic of  
30 gravel-bed rivers.



Water discharge per unit width can be computed by multiplying  $\bar{u}$  by  $h$ :

$$q = \bar{u}h = -\text{sgn}(\alpha)5.9g^{1/2} \frac{h^{5/3}S^{1/2}}{D^{1/6}} \quad (14)$$

Substituting Equation 10 into Equation 14 gives:

$$q = \bar{u}h = -\text{sgn}(\alpha)5.9g^{1/2} \left( \frac{\rho_s - \rho}{\rho} \right)^{5/3} (1 + \epsilon)^{5/3} \tau_c^{*5/3} \frac{D^{3/2}}{S^{7/6}} \quad (15)$$

- 5 The final equation that we require to obtain  $b$  for Equation 2 is that for continuity. We approximate the channel cross-section as rectangular such that the magnitude of the channel-forming water discharge,  $|Q|$ , is equal to the product of the flow speed, width, and depth.

$$|Q| = |\bar{u}|bh = |q|b \quad (16)$$

Rearranging Equation 16 to solve for  $b$ , and then substituting Equation 15 for  $|q|$ , yields:

$$10 \quad b = 0.17g^{-1/2} \left( \frac{\rho_s - \rho}{\rho} \right)^{-5/3} (1 + \epsilon)^{-5/3} \tau_c^{*-5/3} \frac{|Q|S^{7/6}}{D^{3/2}} \\ = k_b \frac{|Q|S^{7/6}}{D^{3/2}} \quad (17)$$

This is the width created by a channel that has a constant ratio of basal Shields stress to critical Shields stress. To focus attention to the variables ( $Q$ ,  $S$ , and  $D$ ), we lump the constants into  $k_b = 2.61$ .

- 15 Finally, channel width ( $b$ ) and sediment discharge per unit width ( $q_s$ , Equation 9) can be multiplied together to yield  $Q_s$ . In order to relate this product to the field, we include an additional term, the intermittency ( $I$ ), which is the fraction of the total time that a river produces a geomorphically-effective flow (after Paola et al., 1992); smaller flows are considered to be unable produce non-negligible geomorphic change. For example, if the annual flood on a self-formed gravel-bed river is a bankfull event, and this event lasts for 3-4 days,  $I \approx 0.01$ ; such conditions are typical for rainfall-fed mid-latitude rivers.

We express this equation first in terms of magnitudes,

$$20 \quad |Q_s| = k_{Q_s} I |Q| S^{7/6}. \quad (18)$$

Then, returning directionality to the equation,

$$Q_s = -k_{Q_s} I |Q| \left| \frac{dz}{dx} \right| \left| \frac{dz}{dx} \right|^{1/6}. \quad (19)$$

In both of these equations,

$$k_{Q_s} = k_{q_s} k_b \\ = \frac{0.17\phi\epsilon^{3/2}}{\left( \frac{\rho_s - \rho}{\rho} \right)^{7/6} (1 + \epsilon)^{5/3} \tau_c^{*1/6}} \\ 25 \quad = 0.041. \quad (20)$$



This demonstrates that in an equilibrium-width river, sediment discharge obeys a stream-power relationship (Paola et al., 1992; Whipple and Tucker, 2002) in which the values of the coefficient and exponents are defined based on the above derivation. Though it is beyond the scope of this work on transport-limited rivers, the derivation of transport capacity to this point may be useful for studies of sediment-flux-dependent detachment-limited river incision (Gasparini et al., 2006, 2007; Hobbey et al., 2011).

Hydraulic geometry adjustment in a threshold-width gravel-bed river results in sediment discharge being independent of grain size. This is the result of a combination of depth to the 5/3 power in the Manning-style equation for water discharge per unit width (Equation 15), the direct proportionality between flow depth and grain size in a threshold gravel-bed channel (Equation 10), flow resistance proportional to grain size to the 1/6 power (Equation 13), and sediment discharge per unit width being proportional to grain size to the 3/2 power (Equation 9, canceling  $D$  out of Equation 19). In more easily visualized terms, the constant excess shear stress ratio maintained by gravel-bed channels (Equation 8) forces channels with larger grains to become narrower, increasing sediment discharge per unit width ( $q_s$ ) but maintaining the same overall sediment discharge ( $Q_s$ ).

In this derivation, we hold  $\tau_c^*$  constant instead of making it a function of slope to the 1/4 power, as has been suggested by Lamb et al. (2008) based on experimental and field data. We do so for three reasons. First, a constant Shields stress is appropriate for rivers with slopes that are  $\lesssim 0.03$  (Lamb et al., 2008); this set comprises most rivers in the world. Second, the assumption of an equilibrium-width river (Parker, 1978) results in the removal of the threshold associated with  $\tau_c^*$  from the sediment-transport equation. Third, the remaining slope dependence is to the 1/24 power (Equation 20). Adding such a weak slope dependence that may marginally improve accuracy would introduce a mathematically significant nonlinearity into the system of equations, thereby impeding our goal of providing intuition into the behavior of gravel-bed rivers.

We combine Equations 1 and 19 with a source/sink term for uplift (or subsidence) to produce a long-profile evolution equation for a transport-limited gravel-bed river.

$$\frac{\partial z}{\partial t} = \frac{Sk_{Q_s} I}{1 - \lambda_p} \left[ \frac{7}{6} \frac{1}{\left(\frac{\partial z}{\partial x}\right)} \frac{\partial^2 z}{\partial x^2} + \frac{1}{Q} \frac{\partial Q}{\partial x} - \frac{1}{B} \frac{\partial B}{\partial x} \right] \left| \frac{Q}{B} \frac{\partial z}{\partial x} \right| \left| \frac{dz}{dx} \right|^{1/6} + U \quad (21)$$

This has the general form of a nonlinear diffusion equation, with the nonlinearity being a combination of  $|dz/dx|^{1/6}$  and any possible nonlinear relationships that arise in  $Q(x)$  and  $B(x)$ . To the right of the equals sign, the leftmost term is a collection of constants. The brackets hold the gradients in slope, water discharge, and valley width. To the right of the brackets are the main drivers: long-profile response rates increase with increasing discharge magnitude and slope, both of which speed sediment transport, and response rates decrease as valley width increases, which creates more space that must be filled or emptied to produce a change in river-bed elevation. This equation would simplify to the linear diffusional relationship derived by Paola et al. (1992) if we (1) considered a constant bed roughness instead of including the Manning-Strickler-based flow resistance that introduces a depth dependence (Equation 13), (2) removed the effects of variable valley width, and (3) considered a uniform water discharge.

Uplift and subsidence ( $U$ ) are not the only possible source and sink for material: Murphy et al. (2016) note the importance of chemical weathering, which must remove mass from rock, and Shobe et al. (2016) investigate the importance of local colluvial



input to rivers. We do not focus on either of these here, but note that the latter must also be related to valley width evolution, which may produce enhanced hillslope sediment inputs, for example, through bank collapse and landsliding.

Equation 21 describes the long-profile evolution of an equilibrium-width gravel-bed alluvial river. The dependencies of the variables in Equation 21 are as follows:

$$5 \quad z = z(x, t) \quad (22)$$

$$Q = Q(x, t) \quad (23)$$

$$B = B(z(x, t), t) \quad (24)$$

$$U = U(x, t) \quad (25)$$

The dependency of valley width,  $B$ , on elevation of the river bed,  $z$ , is the result of the fact that few valleys have vertical walls.

10 Mathematically, this adds an arbitrary dependence on  $z$  that limits the analytically-solvable forms of Equation 21.

## 2.2 Fixed-width river

If the width of the river is externally known and is identical to the width of the valley, another solution is possible. To produce this solution, we first simplify the Exner equation to its one-dimensional form for the case in which  $b = B$  by expanding  $Q_s = q_s b$  and canceling out width:

$$15 \quad \frac{\partial z}{\partial t} = -\frac{1}{1 - \lambda_p} \frac{\partial q_s}{\partial x} \quad (26)$$

Combining this form of the Exner equation with the Wong and Parker (2006) version of the Meyer-Peter and Müller (1948) gravel transport formula, given in Equation 3, and assuming that  $\tau_b^* \geq \tau_c^*$ , leads to the following differential equation for gravel-bed river long-profile evolution:

$$\frac{dz}{dt} = \frac{1}{1 - \lambda_p} \frac{3}{2} \phi \left( \frac{\rho_s - \rho}{\rho} \right)^{1/2} g^{1/2} (\tau_b^* - \tau_c^*)^{1/2} D^{1/2} \left[ D \frac{d\tau_b^*}{dx} + (\tau_b^* - \tau_c^*) \frac{dD}{dx} \right] \quad (27)$$

20 Here, no form of width closure is assumed. We maintain the assumption that  $\tau_c^*$  is a constant, meaning that this equation is valid for rivers of slopes that are  $\lesssim 0.03$  (Lamb et al., 2008). This is done for both comparison with Equation 21 for equilibrium-width rivers and because of the added mathematical complexity of including a weak nonlinearity.

Equation 27 hides discharge, width, slope, and an additional grain-size dependence within  $\tau_b^*$ . To include these explicitly, we combine Equations 16 and 13 to solve for flow depth,  $h$ , and insert this depth into the Meyer-Peter and Müller (1948) sediment  
 25 transport formula (Equation 3) via the definition of dimensionless basal shear stress given in Equation 7:

$$q_s = \begin{cases} 0 & \text{if } |\tau_b^*| \leq \tau_c^* \\ -\text{sgn} \left( \frac{dz}{dx} \right) \phi \left( \frac{\rho_s - \rho}{\rho} \right)^{1/2} g^{1/2} \left( \frac{0.345}{g^{3/10}} \frac{1}{\rho_s - \rho} \frac{1}{D^{9/10}} \left( \frac{|Q|}{b} \right)^{3/5} \left| \frac{\partial z}{\partial x} \right|^{7/10} - \tau_c^* \right)^{3/2} D^{3/2} & \text{if } |\tau_b^*| > \tau_c^* \end{cases} \quad (28)$$

In a natural river,  $q_s$  is combined with an intermittency,  $I$ , which is equal to the fraction of the time that the discharge is geomorphically effective; smaller discharges are assumed to carry negligible bed-load sediment (Paola et al., 1992).



To formulate the differential equation for long-profile evolution of a transport-limited gravel-bed river of arbitrary width, we combine our transport relationship (Equation 28) with our statement of volume balance (Equation 26). In the following equation, we again consider only flows in which  $\tau_b^* > \tau_c^*$ ; to use it in practice, one would first run a check as to whether  $\tau_b^* > \tau_c^*$ . If true, the bed would evolve as shown; if false,  $\partial z / \partial t = 0$ .

$$5 \quad \frac{\partial z}{\partial t} = \frac{3}{2} \frac{\phi g^{1/2} I}{1 - \lambda_p} \left( \frac{\rho_s - \rho}{\rho} \right)^{1/2} \left( \frac{1}{\rho} \frac{0.345}{g^{3/10}} \left| \frac{\partial z}{\partial x} \right|^{7/10} \frac{1}{D^{9/10}} \frac{|Q|^{3/5}}{b^{3/5}} - \tau_c^* \right)^{1/2} D^{1/2} \\
 \left[ \frac{|Q|^{3/5} D^{1/10}}{b^{3/5}} \left| \frac{\partial z}{\partial x} \right|^{7/10} \left( \frac{3}{5} \frac{1}{Q} \frac{\partial Q}{\partial x} - \frac{3}{5} \frac{1}{b} \frac{\partial b}{\partial x} + \frac{7}{10} \frac{1}{\left| \frac{\partial z}{\partial x} \right|} \frac{\partial^2 z}{\partial x^2} - \frac{9}{10} \frac{1}{D} \frac{\partial D}{\partial x} \right) \right. \\
 \left. + \left( \frac{1}{\rho} \frac{0.345}{g^{3/10}} \left| \frac{\partial z}{\partial x} \right|^{7/10} \frac{1}{D^{9/10}} \frac{|Q|^{3/5}}{b^{3/5}} - \tau_c^* \right) \frac{\partial D}{\partial x} \right] + U \quad (29)$$

When  $b$  is set such that Equation 8 for an equilibrium-width gravel-bed channel holds true and  $b = B$ , Equation 29 becomes equal to Equation 21.

In addition to the variable space–time dependencies listed in Equations 22–25, we include the following two for Equation 29:

$$b = b(z(x, t), t) = B(z(x, t), t) \quad (30)$$

$$D = D(x, t) \quad (31)$$

### 3 Analytical solutions

Two analytical solutions are presented here to help build intuition into the shape of gravel-bed river long profiles. The most generally-applicable of these, for an equilibrium-width gravel-bed river that is neither aggrading nor incising in an area with no tectonic activity, is presented first. This solution is a power law that relates measurable hydrologic and landscape parameters to river long-profile shape. The second analytical solution is for a fixed-width river that adds the additional assumptions that width, discharge, and grain size are held constant. This solution provides an equilibrium transport slope.

#### 3.1 Relationships between width, discharge, drainage area, and downstream distance

In order to analytically solve special cases of the provided equations for river channel long-profile evolution, we need a way to write Equation 21 in terms of only  $z$  and  $x$ , meaning that we should rewrite  $Q$  and  $B$  in terms of  $x$ . For any real river, there is a measurable relationship between discharge and distance downstream. Based on observations (Hack, 1957; Costa and O'Connor, 1995; Whipple and Tucker, 1999):

$$|Q| = k_{AQ} A^{P_{AQ}} \quad (32)$$

25

$$A = k_{xA} x^{P_{xA}} \quad (33)$$



$Q$  in Equation 32 refers to the discharge of a geomorphically effective flood – in our case, this is one that applies a shear stress  $\tau_b^* \approx (1 + \epsilon)\tau_c^*$  (Wolman and Miller, 1960; Parker, 1978; Sullivan and Lucas, 2007).  $P_{xA} \approx 4/7$  in the inverse of Hack’s exponent (Gray, 1961; Maritan et al., 1996; Birnir et al., 2001). Substituting  $A$  in Equation 32 with Equation 33 provides the needed transfer function between  $Q$  and  $x$ :

$$5 \quad |Q| = k_{AQ} k_{xA}^{P_{AQ}} x^{P_{xA} P_{AQ}} \quad (34)$$

$$= k_{xQ} x^{P_{xQ}} \quad (35)$$

Solutions to Equation 21 also depend on how valley width,  $B$ , changes with distance downstream. Following Snyder et al. (2000) and Tomkin et al. (2003), who formulated a power-law relationship between valley width and drainage area, we propose that  $B$  is also a power-law function of  $x$ :

$$10 \quad B = k_{xB} x^{P_{xB}} \quad (36)$$

### 3.2 Equilibrium-width river

In order to develop an analytical solution to Equation 21, we first replace  $Q$  and  $B$  with Equations 32–36:

$$\frac{\partial z}{\partial t} = \frac{Sk_{Q_s} I}{1 - \lambda_p} \left[ \frac{7}{6} \frac{1}{\left(\frac{\partial z}{\partial x}\right)} \frac{\partial^2 z}{\partial x^2} + \frac{P_{xQ}}{x} - \frac{P_{xB}}{x} \right] \frac{k_{xQ} x^{P_{xQ}}}{k_{xB} x^{P_{xB}}} \left( \frac{\partial z}{\partial x} \right) \left| \frac{dz}{dx} \right|^{1/6} + U \quad (37)$$

One useful analytical solution to this equation would be that for the steady-state case, in which

$$15 \quad \frac{\partial z}{\partial t} = 0. \quad (38)$$

However, no analytical solution exists for this form of the equation when tectonic uplift or subsidence is present. As a close substitute, and one that can greatly simplify Equation 37, we choose the case in which the river is neither aggrading nor incising. Its only vertical motion, therefore, is as it passively rides up or down on the Earth’s surface.

$$\frac{\partial z}{\partial t} = U \quad (39)$$

20 For the special case in which there is no uplift, equation 38 holds. It is important to note that this case implies a continuous externally-sourced sediment supply in order to maintain a fixed topography without relative uplift across the stream profile.

For such a no-uplift steady-state condition to persist over geologic time requires a constant input of sediment from upstream. This in turn implies that, upstream of the segment of the river for which the analytical solution is calculated, some process is responsible for this constant sediment supply. This could be a constant erosion rate (which can correspond to a constant  
 25 uplift rate in steady state), or perhaps continual supply of gravel-sized sediment from a source outside of the catchment (such as coarse sediment supply by ice caps and ice sheets that can carry gravel across land-surface-defined drainage divides). This steady-state solution may also approximate conditions in a disequilibrium landscape with no tectonic uplift in which the gravel-bed river long profile achieves an equilibrium state over time-scales that are much shorter than changes in sediment supply, which in turn is likely derived from the long-term reduction in landscape relief.



Applying Equation 39 to Equation 37 yields a second-order nonlinear ordinary differential equation that is analytically solvable:

$$0 = \frac{7}{6} \frac{1}{\left(\frac{dz}{dx}\right)} \frac{d^2z}{dx^2} + \frac{P_{xQ} - P_{xB}}{x} \quad (40)$$

Its solution is a law, solved using of two known points  $(x_0, z_0)$  and  $(x_1, z_1)$  on a stream.

$$z = (z_1 - z_0) \left( \frac{x^{(1+6(P_{xB}-P_{xQ})/7)} - x_0^{(1+6(P_{xB}-P_{xQ})/7)}}{x_1^{(1+6(P_{xB}-P_{xQ})/7)} - x_0^{(1+6(P_{xB}-P_{xQ})/7)}} \right) + z_0 \quad (41)$$

The tunable parameter in this power-law solution is  $P_{xB} - P_{xQ}$ . As  $P_{xB}$  may be measured from the landscape, the value of the fit should be able to be related directly to the exponent that describes the downstream increase in geomorphically effective stream discharge.

### 3.3 Fixed-width river

- 10 In order to generate an analytical solution for a fixed-width gravel-bed river, starting from Equation 29, we assume that three key variables are constant: width ( $b = B$ ), water discharge ( $Q$ ), and grain size ( $D$ ). As a result,  $q = Q/b$  is also constant. This may be considered to be a short reach of an incised river with no significant tributaries or a portion of an engineered canal for which discharge varies extremely gradually. Applying these assumptions, and assuming that  $\tau_b^* \geq \tau_c^*$ , produces the following nonlinear diffusion equation with a source/sink (uplift/subsidence) term:

$$15 \frac{\partial z}{\partial t} = \frac{21}{20} \frac{\phi g^{1/2} I}{1 - \lambda_p} \left( \frac{\rho_s - \rho}{\rho} \right)^{1/2} (qD)^{3/5} \left| \frac{\partial z}{\partial x} \right|^{-3/10} \left( \frac{1}{\rho} \frac{0.345}{g^{3/10}} \left| \frac{\partial z}{\partial x} \right|^{7/10} \frac{q^{3/5}}{D^{9/10}} - \tau_c^* \right)^{1/2} \frac{\partial^2 z}{\partial x^2} + U. \quad (42)$$

Solving this equation for the case in which any vertical motion is provided by uplift or subsidence (Equation 39) is a general case of a steady-state long profile ( $\partial z/\partial t = 0$ ) with no uplift or subsidence ( $U = 0$ ). Applying this assumption defines a channel with a uniform slope, where  $(x_0, z_0)$  is a point along the channel long profile,

$$20 z = z_0 - 4.57g^{3/7} \left( \frac{\rho_s - \rho}{\rho} \right)^{10/7} \frac{\tau_c^{*10/7} D^{9/7}}{q^{6/7}} (x - x_0). \quad (43)$$

Slope adjusts to the driving force required to maintain a uniform bed-load sediment discharge. Increasing submerged specific gravity,  $(\rho_s - \rho)/\rho$ , and grain size,  $D$ , resist sediment motion by increasing the weight of the grains, therefore increasing the equilibrium fluvial transport slope. Increasing discharge per unit width ( $q$ ), on the other hand, decreases the equilibrium fluvial transport slope, as this provides more power to move the bed-material sediment.

## 25 4 Numerical solutions

To solve more general cases of Equations 21 and 29, we derive numerical solutions described in Appendix B. The solution to Equation 21 (B3) is solved semi-implicitly by constructing equations with a diffusive component that can be solved directly



in a tridiagonal matrix and a set of nonlinear terms that require Picard iteration. This solution method improves numerical stability and reduces compute times. Python code to solve for the shapes of river long profiles is provided as a snapshot in the Supporting Information and online at <https://github.com/awickert/gravel-river-long-profile>. This library includes functions to analytically solve for the long profile shape as well (Equation 41), and with the proper inputs, this can match the analytical solution (Figure 2).

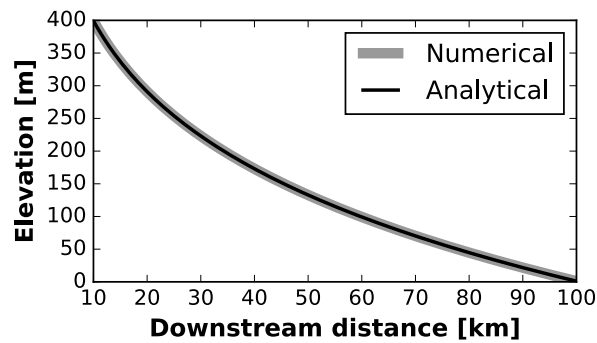


**Figure 2.** When  $dz/dt = U$ , the analytical solution for an equilibrium-width river (Equation 41) matches the numerical solution for an equilibrium-width river (Equation 37). Equation 37 is derived from the general equation for an equilibrium-width river, Equation 21, to include power-law downstream relationships for valley width and water discharge (Equations 32–36). Here, the slope at the upstream boundary condition is  $S_0 = 0.015$ ; this is set to produce an input bed-load sediment discharge of  $Q_{s_0} = 3.48 \times 10^{-4} \text{ m}^3 \text{ s}^{-1}$ . Water discharge,  $Q = 1.43 \times 10^{-5} x^{49/40} \text{ m}^3 \text{ s}^{-1}$ ; drainage area,  $A = x^{7/4} \text{ m}^2$ , and valley width,  $B = 25x^{1/5} \text{ m}$ .

## 5 Discussion

### 5.1 Parameterizing stream-power-based sediment discharge

Whipple and Tucker (2002, Equation 4) posited that sediment discharge should follow the power-law relationship

$$Q_c = K_t A^{m_t} S^{n_t}, \quad (44)$$

10 where  $Q_c$  is the bed-load sediment transport capacity and is equal to  $Q_s$  for transport-limited rivers,  $K_t$  is a coefficient,  $A$  is drainage area, and  $m_t$  and  $n_t$  are exponents. Howard and Kerby (1983) and Willgoose et al. (1991) present arguments for  $m_t = n_t = 2$  for sand-bed rivers, and Whipple and Tucker (2002) posit that  $n_t = 1$  for gravel-bed rivers.

The sediment-transport formulation that we present in Equation 19, when combined with the discharge to drainage area relationship of Equation 32 and dropping references to directionality, can be rewritten in a way that is analogous to the above  
 15 equation for  $Q_c$ :

$$Q_c = k_{Q_s} k_{AQ} I A^{P_{AQ}} S^{7/6} \quad (45)$$



This relationship provides a value for  $n_t$ , based on experiments and theory (Meyer-Peter and Müller, 1948; Parker, 1978; Wong and Parker, 2006). It also provides a likely range of values for  $m_t$  based on empirical studies that relate drainage basin area to geomorphically-effective discharge. Furthermore, it defines a starting point towards quantifying the free parameter  $K_t$ :  $k_{Q_s} = 0.041$  is known (Equation 20),  $I$  relates to the variability of the hydrograph, and  $k_{AQ}$  must relate to precipitation patterns across the drainage basin. We therefore focus on understanding the power-law discharge–drainage-area scaling ( $k_{AQ}$  and  $P_{AQ}$ ), as solving this would constrain or define the remaining constants in Equation 45 and allow us to relate slope and drainage area, easily measured from digital elevation models (DEMs), directly to gravel transport capacity.

The appropriate value of  $P_{AQ}$  depends on the flow of interest. For mean flow in a basin that experiences uniform precipitation, it is 1 (given catchment-wide water balance). For more rare flows,  $P_{AQ} < 1$ . This is because smaller basins may be completely covered by a storm event, leading to a catchment-wide response to a unit hydrograph, but larger basins may not have coherent storms across the whole basin, leading to attenuation of flood peaks and a decrease of the likelihood of a flood that is as large a ratio of the mean flow as in the small basin (Aron and Miller, 1978; Snow and Slingerland, 1987; Milly and Eagleson, 1988). Aron and Miller (1978) found that, for annual flood peaks in  $\sim 50$  streams in Pennsylvania and New Jersey (USA),  $P_{AQ} \approx 0.7$ ; such annual floods are generally also those that move gravel. Whipple and Tucker (1999) suggest values of 0.7–1.0 for bedrock erosion, and Sóllyom and Tucker (2004) find that  $1/2 \leq P_{AQ} \leq 1$ , which is in agreement with field data from Strahler (1964, p. 50). The lower limit from Sóllyom and Tucker (2004) is for a single storm that whose duration is  $\ll$  its travel time through the basin. O'Connor and Costa (2004) used the entire U.S. Geological Survey gauging history (Slack and Landwehr, 1992) to compute that, on average,  $P_{AQ} = 0.57$  for 90th-percentile floods and  $P_{AQ} = 0.53$  for 99th-percentile floods.

We normalize  $A$  to a characteristic footprint area of storms that occur across the catchment over the time scale of interest,  $A_R$ , and assume that  $A \geq A_R$  for transport-limited gravel-bed rivers:

$$Q_c = k_{Q_s} I q_R A_R \left( \frac{A}{A_R} \right)^{P_{AQ}} S^{7/6}. \quad (46)$$

This definition applies the power  $P_{AQ}$  to a dimensionless ratio, thereby ensuring that the coefficients can be framed in terms of rainfall. Here, we define a new coefficient that is the rainfall rate (i.e. flux) during a specific set of coincident rainfall events,  $q_R$ ;  $k_{AQ} = q_R A_R^{1-P_{AQ}}$ . For simplicity, we do not consider inefficiencies in rainfall-to-discharge conversion, though factors could be added to an analogous expression to represent evapotranspiration and/or groundwater loss to other catchments.

From this relationship, we can assign values to the following parameters from Whipple and Tucker (2002):

$$K_t = k_{Q_s} I q_R A_R^{1-P_{AQ}} \quad (47)$$

$$m_t = P_{AQ} \quad (48)$$

$$n_t = 7/6 \quad (49)$$

For example, picking a characteristic storm footprint of  $100 \text{ km}^2$ ,  $P_{AQ} = 7/10$  (after Aron and Miller, 1978), and  $q_R = 1 \text{ cm hr}^{-1}$ , we find that  $K_t \approx 2 \times 10^{-5} \text{ m}^{2/7} \text{ s}^{-1}$ ,  $m_t = 7/10$ , and  $n_t = 7/6$ .



## 5.2 Concave-up long profiles require weathering and/or downstream fining

Whipple and Tucker (2002) proposed that at steady state, sediment discharge should be proportional to uplift times contributing area. We make the modification that contributing area must be raised to a power,  $0 \leq P_\beta \leq 1$ , that we term the “gravel persistence exponent”. This describes the persistence of gravel-sized particles as they are weathered through hillslope processes (Attal et al., 2015; Sklar et al., 2017) and/or fine downstream (Sternberg, 1875; Attal and Lavé, 2009; Dingle et al., 2017). If  $P_\beta = 1$ , every piece of eroded material on the landscape becomes gravel that reaches the stream. Considering that fluvial gravels have round edges and therefore cannot pack together without void space, this is topologically impossible. If  $P_\beta = 0$ , all material weathers on the hillslope before it reaches the stream. Intermediate values of  $P_\beta$  indicate that some combination of hillslope weathering and downstream fining reduce the gravel supply to a nonzero fraction of the initially-eroded material.

$$10 \quad Q_s = \beta A^{P_\beta} U. \quad (50)$$

By assuming that channels are transporting sediment at capacity and that most transport-limited gravel-bed rivers should have gravel banks and exist at a threshold state, we can equate this to Equation 45 and rearrange the terms to create a slope–area relationship:

$$S = \left( \frac{\beta U}{k_{Q_s} k_{AQ}} \right)^{6/7} A^{(6/7)(P_\beta - P_{AQ})}. \quad (51)$$

15 In order for a river at steady state to have a concave long profile, meaning that channel slope decreases as drainage area increases (as is observed in nature), the exponent to which drainage area ( $A$ ) is raised must be negative. This slope–area exponent, multiplied by  $-1$ , is defined as the concavity index,  $\theta$ , (Whipple and Tucker, 1999):

$$S = k_s A^{-\theta}. \quad (52)$$

Here,  $k_s$  is the channel steepness index (Moglen and Bras, 1995; Sklar and Dietrich, 1998; Whipple, 2001).

20 In the case of Equation 51,  $\theta = -(6/7)(P_\beta - P_{AQ})$ . If  $P_\beta = 1$ , as assumed by Whipple and Tucker (2002, Equation 7b), and  $0.5 \leq P_{AQ} \lesssim 0.7$ , as prior work has demonstrated (Aron and Miller, 1978; Snow and Slingerland, 1987; Whipple and Tucker, 1999; O’Connor and Costa, 2004), then the exponent to which  $A$  is raised would become positive. Such a river would be required to have a downstream-increasing slope in order to transport the sediment that it is supplied. This would result in a convex steady-state long profile, which is not observed in nature.

25 These assumptions produce a convex long profile because as drainage area increases, sediment supply increases more strongly than water discharge. A straightforward solution is to adjust  $P_\beta$ , which describes the attenuation rate of gravel-sized particles with increasing drainage area. As drainage area increases, so does the mean transport distance of a particle that reaches the corresponding point on the stream. As transport distance increases, so does the possibility of significant weathering on the hillslope or breakdown in the channel (Attal and Lavé, 2009; Attal et al., 2015; Sklar et al., 2017; Dingle et al., 2017). This combination of weathering and downstream fining can significantly reduce the amount of gravel-sized sediment supplied to a channel cross-section as drainage area increases.

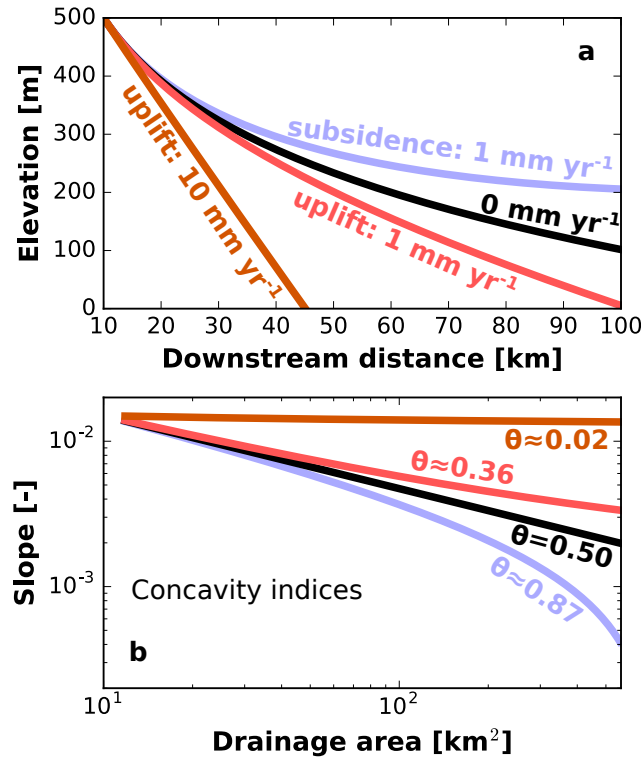


**Figure 3.** Steady-state numerical model outputs with steady uplift (base-level fall), subsidence (base-level rise), or neither. These numerical solutions are formulated following Equation B3, which is a finite-difference discretization of the general equation for an equilibrium-width transport-limited gravel-bed river, Equation 21. Power-law relationships describe downstream increases in water discharge ( $Q$ ) and valley width ( $B$ ), following Equations 32–37. (a) Long profiles. (b) Slope-area plots: concavities increase with increasing subsidence. All channels are plotted such that they are pinned to the same upstream point. Model input parameters other than uplift are the same as those given for the long profiles displayed in Figure 2.

An approximate value for the gravel persistence exponent,  $P_\beta$ , can be calculated by noting that in most natural rivers,  $\theta \approx 0.45$  to  $0.5$ . Combining this with the observation that  $0.5 \leq P_{AQ} \lesssim 0.7$  leads to the result that  $P_\beta \lesssim 0.2$ . This low gravel persistence exponent implies rapid attenuation of gravel-sized sediment as drainage area increases: doubling of drainage basin area would produce a  $<15\%$  increase in the volume of gravel-sized sediment supplied to a channel cross-section. For break-

5 down of clasts within the fluvial system, this is qualitatively consistent with the observation by Dingle et al. (2017) that gravel is entirely absent from Himalayan rivers starting 10–40 km from where they enter the Ganga Plain, the point at which gravel inputs terminate.

Figure 3 indicates that uplift can act to reduce the concavity in the downstream direction. This increases the fraction of the eroded landscape that acts to produce gravel, which is intuitively consistent with the implicit reduced residence time of soils on

10 hillslopes, and presumably the shorter time available to weather into fine sediment (Attal et al., 2015). As increasing rates of uplift (or base-level fall) force the channel long profile to become straight (concavity  $\theta = 0$ ), the gravel persistence exponent,



$P_{\beta}$ , increases to equal the drainage-area-to-discharge exponent,  $P_{AQ}$ ; constant channel slope requires a constant ratio of water to sediment discharge.

The small value of  $P_{\beta}$  significantly increases the critical drainage area for the transition between from a detachment-limited channel to a transport-limited channel (Whipple and Tucker, 2002). This is because increasing drainage area does not increase sediment supply as rapidly as assumed by (Whipple and Tucker, 2002). Therefore, a relatively larger portion of the landscape may be assumed to be detachment-limited than previously thought.

### 5.3 Concave-up long profiles require valley widening

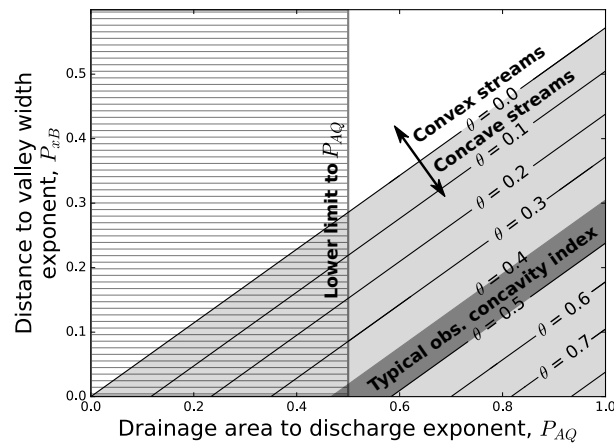


**Figure 4.** The slope–area concavity index defined in Equations 52 and 55 limits the range of possible powers for discharge–drainage-area and width–distance relationships. The light gray field includes all concave long profile solutions, and the dark gray indicates where the concavity index is in a commonly-observed range for rivers in the field, between 0.4 and 0.5. The hatched area on the left is below the theoretical lower limit for the exponent that relates drainage area to water discharge,  $P_{AQ} = 0.5$ , which exists in the limit where storm duration is much less than the time for that water to pass through the catchment (Sólyom and Tucker, 2004). This example is given for an equilibrium-width river for which  $dz/dt = U$ , which corresponds to the analytically-solvable case in Equations 40 and 41.

Equation 40 for a steady-state river with neither uplift nor subsidence can be rewritten with  $dz/dx$  replaced by  $S$  and  $P_{xQ}$  replaced by its constituent components  $P_{xA}$  and  $P_{AQ}$ :

$$10 \quad \frac{7}{6} \frac{1}{S} \frac{dS}{dx} = \frac{P_{xB} - P_{xA}P_{AQ}}{x} \quad (53)$$

In order to solve this equation, we rely on the fact that at the upstream boundary condition,  $x = x_0$  and  $S = S_0$ . Here, the slope is set to prescribe the input sediment discharge,  $Q_{s_0}$ , in a way that is independent of the water discharge (see Equation 19). We solve Equation 53 to obtain a slope–distance relationship,

$$S = S_0 \left( \frac{x}{x_0} \right)^{(6/7)(P_{xB} - P_{xA}P_{AQ})} \quad (54)$$



We then substitute drainage area,  $A$ , for  $x$  based on an inversion of Equation 33:

$$S = S_0 \frac{k_{xA}^{(6/7)(P_{AQ} - P_{xB}/P_{xA})}}{x_0^{(6/7)(P_{xB}/P_{xA} - P_{AQ})}} A^{(6/7)(P_{xB}/P_{xA} - P_{AQ})} \quad (55)$$

Based on Equation 55, the concavity index (Equation 52) is  $\theta = (6/7)(P_{AQ} - P_{xB}/P_{xA})$ , and the steepness index,  $k_s$  is equal to the terms forming the coefficient before the  $A$  term. For a characteristic inverse Hack's exponent ( $P_{xA} = 7/4$ ) and range of likely concavity index values,  $0.4 \lesssim \theta \lesssim 0.5$ , a tight bound exists on the possible values of  $P_{AQ}$  and  $P_{xB}$  (Figure 4). These values span the range of observed (Aron and Miller, 1978; Howard and Kerby, 1983; Whipple and Tucker, 1999) and theoretical (Sólyom and Tucker, 2004) steady-state river concavity index values. Furthermore, this formulation demonstrates that a downstream-widening valley can be necessary to produce rivers of observed concavity index values for common values of  $P_{AQ}$ . Insofar as valley widening can be recognized in the field, this observation can be used in areas of little to no uplift to connect geomorphic form directly to the area scaling relationship for a dominant river discharge (Figure 4, dark gray diagonal region).

#### 5.4 Signatures of change in sediment-to-water supply ratio (climate) and/or base level (tectonics)

One major aim of fluvial geomorphology is to interpret changing environmental forcing from the shape of river long profiles. The two major controls on transport-limited river channel long-profile evolution are the ratio between water and sediment supply (e.g., Parker et al., 1998), which drives the upstream flux boundary condition, and changes in the relative elevation between the river and its base-level, which drive the downstream boundary condition (Hilley and Strecker, 2005). The upstream boundary condition may be driven by changes in climate (Tucker and Slingerland, 1997; Simpson and Castelltort, 2012); tectonics, which by modifying topographic relief can influence sediment supply and grain size (Attal et al., 2015; Sklar et al., 2017); or by other factors – including humans – that impact water and/or sediment delivery to rivers (e.g., Liébault and Piégay, 2001). The downstream boundary condition is defined as a relative change, and therefore may be driven by (1) rise and fall of the river outlet (Faulkner et al., 2016) and/or (2) uplift or subsidence of the solid Earth beneath the river (Paola et al., 1992; Whipple and Tucker, 2002; Johnson et al., 2009).

Here we demonstrate that transport-limited gravel-bed rivers adjust their steepnesses to the sediment-to-water input ratio (Figure 5d,e; associated response time in Figure 6d,e) and adjust their concavities to uplift rate (i.e. relative changes in base level: Figures 3, 5b,c), and 6b,c) with an amplitude that is controlled in part by sediment supply. These distinct modes of response allow us to distinguish whether the upstream (flux) boundary condition or the downstream (base level) boundary condition, or both, are controlling the river long-profile shape. Over short time scales, this river-profile adjustment could relate to natural or anthropogenic changes in water and sediment supply, as well as changes in base level due to, for example, sea-level change, glacial-isostatic adjustment, reservoir construction, or dam removal. Importantly, many such natural base-level changes also change the horizontal position of the river outlet, and the overall river response is due to both horizontal and vertical changes in outlet position, even though we discuss only an idealized vertical base-level change here. Over geologic time scales, such river adjustments may record climate and/or tectonics, and the equilibrium long-profile shape is a function of the competition between tectonics – uplift adds material to the river profile and subsidence takes it away – and the incoming

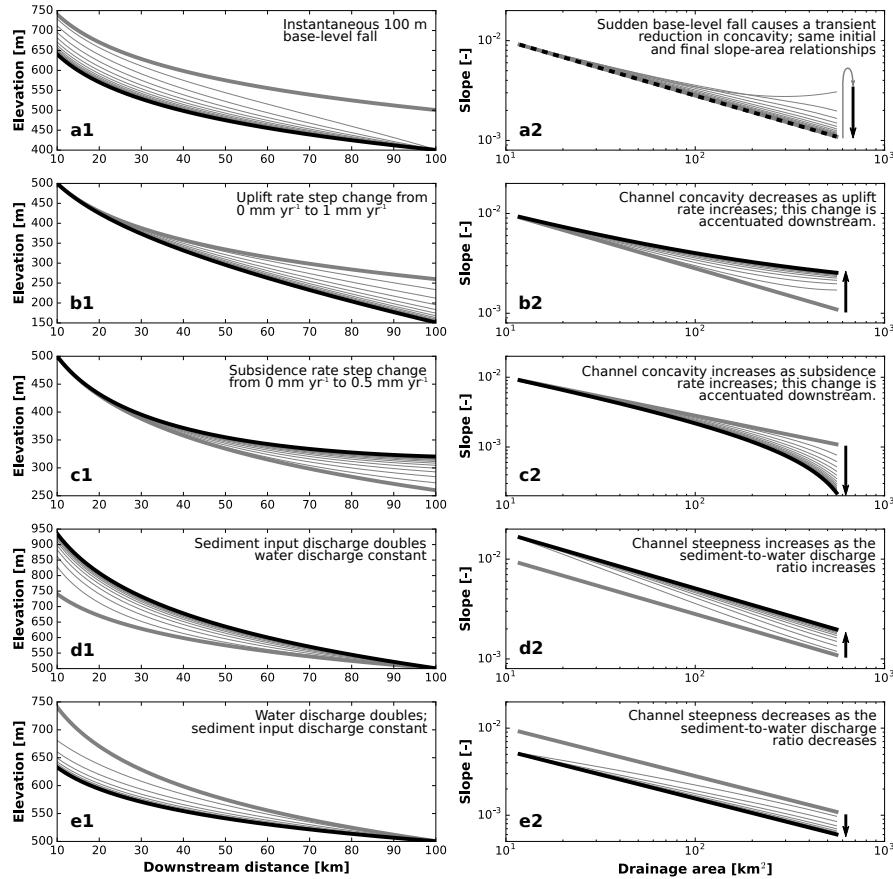


**Figure 5.** Transient long profiles from numerical model runs. Base model boundary conditions and parameters  $S_0 = 0.01$ ;  $10 \text{ km} \leq x \leq 100 \text{ km}$ ;  $Q = 1.43 \times 10^{-5} x^{49/40} \text{ m}^3 \text{ s}^{-1}$ ;  $A = x^{7/4} \text{ m}^2$ ,  $B = 79.06 x^{1/10} \text{ m}$ . Each fine gray line represents 30,000 years with an intermittency of  $I = 1$  (i.e. constant geomorphically-effective discharge conditions). All base-level changes are purely vertical, and therefore can represent steeply-dipping faults or sea-level change across a steep coastline. **(a)** An instantaneous 100 m base-level fall causes a transient response but eventually produces the same channel long profile, albeit translated downward. **(b)** The onset of  $1 \text{ mm yr}^{-1}$  steady base-level fall (or tectonic uplift) reduces channel concavity; this allows the river to transport the additional bed-derived sediment as it incises. **(c)** The onset of  $0.5 \text{ mm yr}^{-1}$  steady base-level rise (or subsidence) increases concavity due to increasing deposition rates that are required to fill the accommodation space created. **(d)** Doubling the input sediment discharge ( $Q_{s0}$ ), facilitated by adjusting  $S_0$  according to Equation 19, increases channel steepness proportionally (Equation 55); this increase in steepness propagates downstream. **(e)** Doubling the water discharge ( $Q$ ) decreases channel steepness proportionally; this decrease in steepness propagates downstream more rapidly than that due to doubling sediment input because an increase in water discharge increases sediment transport capacity.

sediment discharge that sets the pace at which the river can remove uplifting sediment or deposit sediment in a region of subsidence.

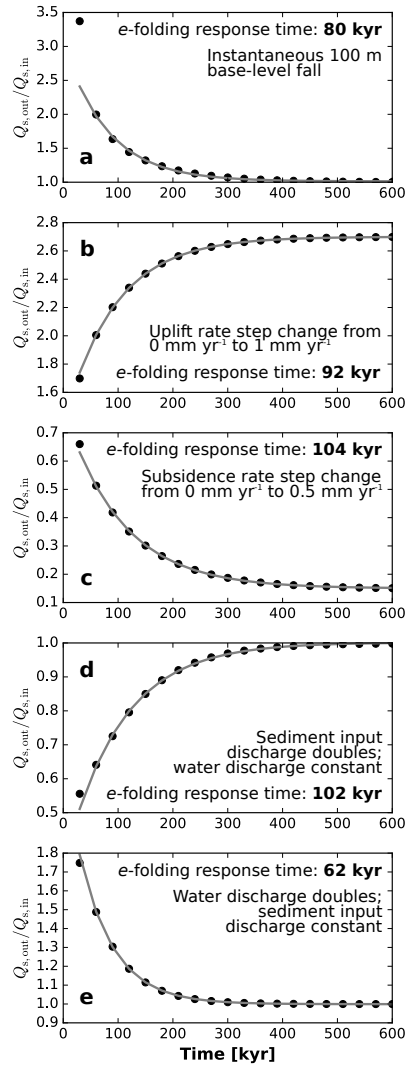


**Figure 6.** Transient response and response times to external forcings as quantified by the ratio of sediment input to output discharge. Each dot on this figure corresponds to a gray line on the panels of Figure 5 bearing the same letter. **(a)** A sudden increase in sediment flux following a sudden base-level fall event gradually decays until the sediment output is equal to the sediment input. **(b)** Sediment output rises to accommodate the additional material supplied at the river bed by tectonic uplift. **(c)** Sediment output falls in response to subsidence, which creates accommodation space for local storage in the subsiding valley floor. **(d)** Doubling input sediment discharge gradually leads to channel steepening and an increase in output sediment discharge. **(e)** Doubling water discharge leads to a decrease in channel steepness and an increase in output sediment discharge; the river responds faster than if sediment input were doubled (d) because increasing water discharge drives a higher sediment transport capacity (Equation 19). We quantify these relationships with exponential decay functions and an *e*-folding time scale, but note that this does not describe the changes in sediment discharge immediately following the perturbation.



#### 5.4.1 Sediment-to-water discharge ratio determines channel steepness

Changes in the input sediment-to-water discharge ratio, in the absence of changes in uplift rate (or equivalently, rate of base-level change), determine the steepness index of a channel but do not affect its concavity (Equations 52 and 55). As the input sediment-to-water discharge ratio increases, the channel steepens in order to transport the additional sediment load out of the system at the rate that it is supplied (Figures 5d and 7). This increase in steepness and associated aggradation is sourced at the headwaters (i.e. the location of the sediment and water source) and propagates downstream. Conversely, a decrease in input sediment-to-water discharge ratio causes a downstream-propagating decrease in steepness (Figure 5e). The time scale of slope response can be approximated as an exponential decay fit to the ratio of output to input sediment discharge, which results from a change in the amount of sediment stored within the system (Figure 6d,e). Changing the sediment-to-water discharge ratio requires adjusting the virtual slope at the upstream boundary ( $S_0$ ). Thus, this steepening can also be viewed as the natural result of requiring the solution to the equation for the long profile to accommodate a steeper upstream gradient boundary condition.

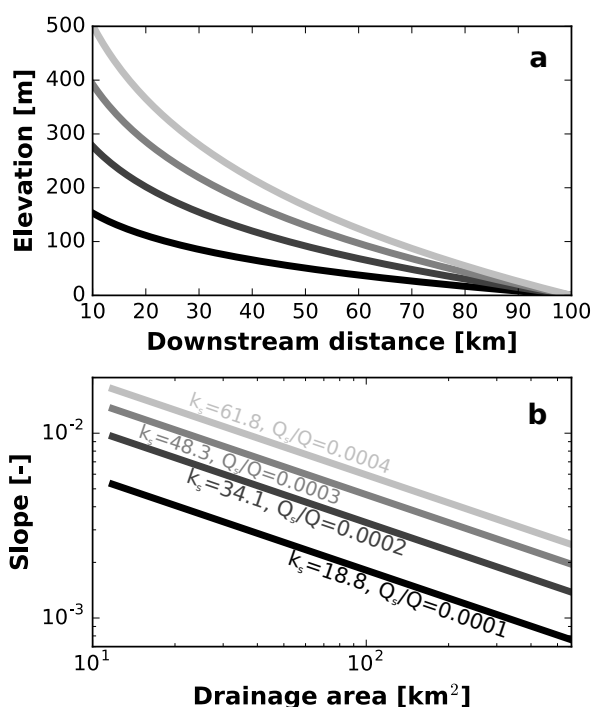


**Figure 7.** As sediment-to-water discharge ratio increases, a steeper channel is required to mobilize the sediments, and as a result, the channel steepness index ( $k_s$ , Equation 52) increases.



#### 5.4.2 Tectonic uplift and subsidence modulate river concavity

With a constant incoming sediment-to-water discharge ratio, changes in the rate of base-level rise or fall, including those caused by tectonic subsidence or uplift, modify the concavity but not the steepness of a transport-limited gravel-bed river long profile (Figure 3). Rivers experiencing tectonic subsidence (base-level rise) will have more concave steady-state long profiles than those with no uplift or subsidence, and those experiencing uplift (base-level fall) will have straighter (less concave) long profiles (Figure 3). This can be understood as follows: base-level rise "pushes" the bottom of the river profile upwards, bending it, while base-level fall "pulls" the bottom of this curve downwards, straightening it.

The analytical solution (Equation 41) provides a long profile in the absence of uplift or subsidence ( $dz/dt = 0$ ). This solution follows the black line in Figure 3 and can be a useful reference case for against which to compare numerical solutions of long-profile shape. Numerical solutions, on the other hand, demonstrate deviations in long-profile shape from this reference case in response to nonzero uplift and/or subsidence.

Even though water-to-sediment discharge ratio cannot on its own impact long-profile concavity, it can (through volume balance) influence degree to which uplift (or subsidence) do. Uplift or subsidence add or remove material from the bed of the river, and changes in concavity are the river's response to redistribute sediment discharge to balance these local sources or sinks of sediment. If the sediment discharge of the river is large compared to the amount of material moved by uplift or subsidence, then only a small adjustment of concavity is necessary to balance this source (uplift) or sink (subsidence) and maintain steady-state topography. A river carrying very little sediment, however, will have to dramatically change its long-profile concavity in order to reach steady state. Therefore, the steady-state long-profile concavity results from a competition between tectonics and sediment discharge, in which a channel-concavity change is induced by a tectonic (or base-level) forcing, but is dampened by increasing sediment input.

In order to compare both sediment discharge and uplift as velocity scales, we define a characteristic alluvial response rate as the incoming sediment discharge from all tributaries ( $Q_{s_{in}}$ ), divided by the area of the valley floor, which equals the mean valley width ( $\bar{B}$ ) multiplied by the length of the study river segment ( $L$ ). We term this alluvial response rate  $\mathbb{A}$ , and it has units of length per time:

$$\mathbb{A} = \frac{Q_{s_{in}}}{L\bar{B}}. \quad (56)$$

Deviations in concavity from a no-uplift state are amplified as the ratio of uplift rate to alluvial response rate increase.

We note that  $Q_{s_{in}}$  is only equal to the incoming sediment discharge at the upstream boundary condition,  $Q_{s_0}$ , for the case in which there are no tributaries. When implicitly considering tributary inputs of water and sediment, as we do for any nonzero  $P_{xA}$  and  $P_{xQ}$ , the total sediment input can be calculated by imposing a steady-state assumption with no uplift, which requires that the total sediment output must equal the sediment input. This can be calculated using Equation 19, with discharge at the downstream boundary known, and the slope at the downstream boundary calculated using Equation 54.

Dividing the tectonic uplift (or subsidence) rate ( $U$ ) by the alluvial response rate ( $A$ ) provides a dimensionless number that defines the relative importance of sediment discharge vs. tectonics in determining the concavity of transport-limited gravel-bed

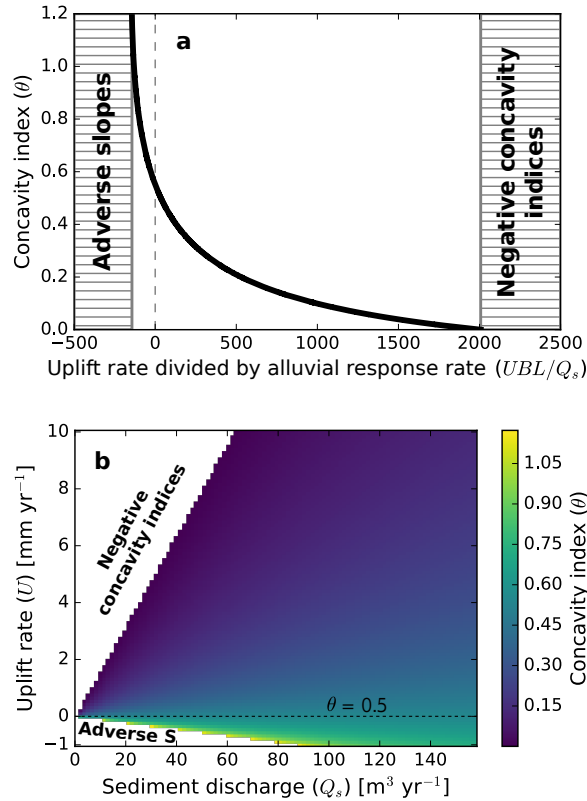


**Figure 8.** Concavity changes uplift (or subsidence) rates increase when compared to a characteristic alluvial response rate. **(a)** As in Figure 3, increasing uplift rates decrease the channel concavity index. Here we vary channel width, sediment discharge, and uplift, and demonstrate how channel concavity change follows the ratio of uplift rate, the external driver, to the internal system response rate (Equation 57). We disallow solutions that produce adverse slopes (these occur with high subsidence) or negative concavity indices (these occur with high uplift rates), as the former break the assumptions of our equations and the latter are not observed steady-state forms in nature. Changes in the valley width exponent,  $P_{xB}$ , change the shape of this curve by changing the downstream distribution of valley widths and therefore altering the local alluvial response rates; all calculations for both panels were performed using  $P_{xB} = 1$ . **(b)** For a single mean valley width (177 m), we compare concavity index against the ratio of sediment discharge to uplift rate. It is important to note that with no uplift, concavity is constant at  $\theta = 0.5$  regardless of sediment discharge.

ivers.

$$\frac{U}{\mathbb{A}} = \frac{LBU}{Q_s} \quad (57)$$

As this ratio becomes more positive, concavity decreases; as it becomes more negative, the concavity decreases. Uplift (or subsidence) rate determines the existence and sign of the concavity change, whereas the ratio of uplift rate to alluvial response



rate determines the magnitude by which concavity deviates from a reference value for a river that experiences no uplift; in Figure 8, this value is 0.5.

Rivers also exhibit a transient response to changes in base level at a rate that is proportional to the alluvial response rate,  $\Delta$  (Equation 56). A single sudden change in base level generates a diffusive wave of incision (Figure 5a1) or aggradation. This wave propagates upstream until the channel achieves the same slope and concavity as it did prior to the incision or aggradation event (Figure 5a2), just at a different absolute elevation. A change in the rate of base-level change over time (through, for example, a change in tectonic uplift or subsidence rate) propagates upstream and changes the concavity of the river (Figure 5b,c). We characterize the time scale of this response in terms of the ratio of the input vs. output sediment flux. When this ratio is less than unity, the river valley is storing sediment, and when it is greater than unity, it is releasing sediment. This change in sediment storage produces a disequilibrium change in the long-profile shape. The first stage of response to a perturbation does not follow a simple pattern, but following this, an exponential decay function can describe the approach to a new equilibrium state. This allows us to define an  $e$ -folding response time that approximates the time required for a river system to respond to a perturbation (Figure 6).

### 5.4.3 Feedbacks between sediment supply and tectonics

In the above section, we have just separated the effects of tectonics and climate as concavity and steepness responses, respectively. Our concavity changes derived from theory and their causes are generally consistent with the broad range of concavities and causes thereof synthesized by Whipple (2004, p. 161), albeit for bedrock rivers. However, such observations do not preclude a potential feedback by which increasing tectonic uplift rates may also increase gravel-sized sediment supply to the channel. In other words, the simplified approach of “climate = water-to-sediment supply, tectonics = base level” may be over-simplified.

Section 5.2 indicates that as uplift rates increase, the landscape surrounding the channel system steepens and erodes (Roering et al., 1999). Our above solutions for changes in tectonic uplift rates (Figures 5b and 6b) require only that the channel excavates the additional sediment from the bed of its valley. This does not include additional sediments from the surrounding hillslopes, and steeper landscapes (often resulting from tectonic uplift) may be expected to produce a larger fraction of coarse material through landsliding and a shorter residence for weathering in the shallow subsurface (Attal et al., 2015; Carretier et al., 2015; Schildgen et al., 2016; Sklar et al., 2017). Changing gravel supply can dramatically alter river long profiles (Savi et al., 2016), and therefore an increase in tectonic uplift rate may lead to both an increase in channel steepness that is not related to climate and a dampened decrease in concavity due to the increase in incoming bed-load sediment discharge that increases the alluvial response rate,  $\Delta$  (Figure 9). This tight channel–hillslope linkage challenges the paradigm that channel incision rates control hillslope morphology and motivates future work into models of landscape evolution that track and conserve sediment (Shobe et al., 2016; Sklar et al., 2017).

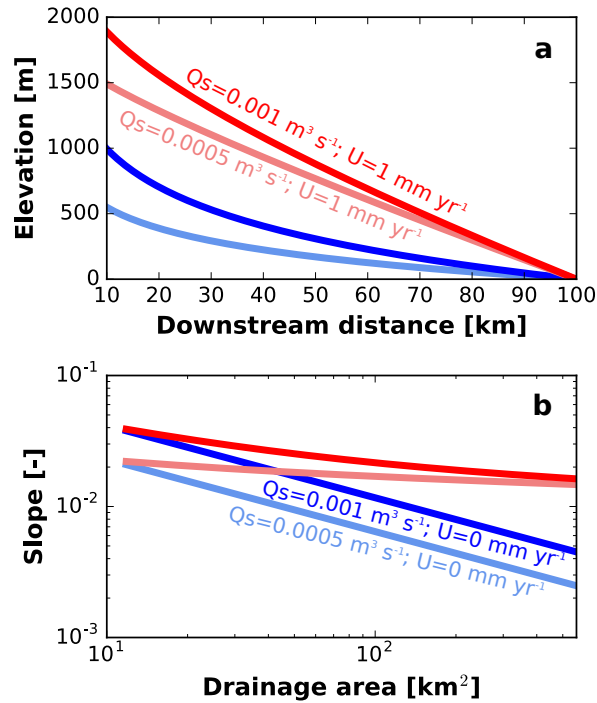


**Figure 9.** Covarying tectonic uplift (or base-level fall) and input sediment-to-water supply ratio produces a range of channel long profiles (a) and steepness and concavity indices (b). It is likely that sediment supply increases with tectonic uplift, and therefore that the variables controlling both the upstream and downstream boundary conditions may change at the same time.

### 5.5 Concavity and downstream fining required for $b \propto Q^{1/2}$

It has long been recognized that river channel width scales with discharge to the  $1/2$  power,

$$b \propto Q^{1/2}. \quad (58)$$

This observation has been confirmed by a century of field studies (Lacey, 1930; Leopold and Maddock, 1953; Hey and Thorne, 1986; Singh, 2003). It has also been the subject of theoretical approaches to determine the static shape of a river channel (Savenije, 2003; Millar, 2005). Here we derive a physically-based reason for this observation for an equilibrium-width gravel-bed river.

Equation 17 relates the width of an equilibrium-width gravel-bed river to discharge, slope, and grain size. Starting with Equation 17, a slope–area relationship of  $S = k_s A^{-\theta}$  (Equation 52), and the drainage-area–discharge relationship from Equation 32, one can write that

$$b = k_b k_s^{7/6} k_{AQ}^{(7/6)\theta/P_{AQ}} \frac{Q^{1-(7/6)\theta/P_{AQ}}}{D^{3/2}}. \quad (59)$$



This demonstrates that channel width is controlled by water discharge, channel concavity (through the concavity index) and downstream fining. Assuming a tight bound on channel concavity, as is generally assumed and has been observed in bedrock channels in the field (Duvall, 2004), though not universally (Whipple, 2004), two main drivers remain: water discharge and downstream fining (Figure 10). Increasing water discharge can cause the channel to widen by requiring more space for the water to flow. Decreasing bed-material grain size reduces the critical Shields stress for initiation of motion, and in order for an equilibrium-width channel to maintain a constant ratio of applied to critical Shields stress, the channel slope must become gentler and/or the channel itself must become wider. Due to the aforementioned tight bounds on concavity index, the rate at which the channel slope decreases is also fixed, and any additional channel response to downstream fining must occur through channel widening.

Combining Equations 58 and 59 and simplifying the result produces a solution for a power that relates grain size to discharge,  $P_{DQ}$ . This demonstrates how grain size must vary downstream in order to maintain the observed channel-width–discharge relationship:

$$D \propto Q^{(3-7\theta/P_{AQ})/9}. \quad (60)$$

Therefore,

$$P_{DQ} = \frac{3}{9} - \frac{7}{9} \frac{\theta}{P_{AQ}}. \quad (61)$$

The range of physically permissible values for the exponent that relates drainage area to discharge,  $P_{AQ}$ , is 0.5–1.0 (Costa and O’Connor, 1995; Solyom and Tucker, 2004). Combining this range of values with a typical concavity index of  $\theta = 0.5$  produces bounds on the exponent in Equation 60 of  $-4/9 \leq P_{DQ} \leq -1/18$ : all plausible solutions require downstream fining to occur in order to reproduce the observed channel-width–discharge relationship (Lacey, 1930).

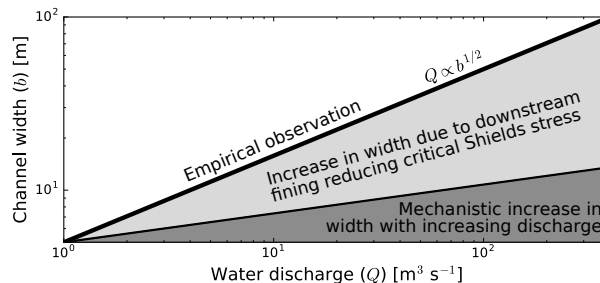


**Figure 10.** In an equilibrium-width self-formed gravel-bed river channel, the common field observation that river channel width is proportional to the square root of water discharge may be explained by a combination of the direct impact of river discharge on channel width and by downstream fining of bed-material sediment.

Using standard values of  $\theta = 0.5$  and  $P_{AQ} = 0.7$  (for a one-year flood Aron and Miller, 1978), one finds that  $b \propto Q^{1/6} D^{-3/2}$ . In this case, in order to recover the empirical  $b \propto Q^{0.5}$  relationship,  $D$  must be proportional to  $Q^{-2/9}$ . Testing this prediction



against downstream fining data, requires that we convert discharge ( $Q$ ) to distance downstream ( $x$ ). While Sternberg (1875) provides reasoning to expect an exponential decay of grain size with distance downstream from a source area, this may be approximated by a power-law function. Multiplying  $P_{AQ} = 0.7$  by the inverse Hack's exponent  $P_{xA} = 7/4$  (Equation 35) produces the multiplier to convert the grain-size–discharge relationship to a grain-size–downstream-distance relationship:  $D \propto x^{0.27}$ . We have performed no rigorous analysis of this result, but data from Gomez et al. (2001) from the braided Waipoa River in New Zealand are broadly consistent with this exponent.

## 6 Conclusions

We have produced equations to describe the long-profile evolution of transport-limited gravel-bed rivers by combining the Exner equation for conservation of volume, the Wong and Parker (2006) modification of the (Meyer-Peter and Müller, 1948) formulation for gravel transport, a Manning-style flow resistance equation (Parker, 1991), the normal-flow approximation for basal shear stress, the channel-width closure of (Parker, 1978), and the continuity equation. The key equation of this paper is Equation 21, which captures the dynamics of a gravel-bed river whose bed shear stress is a multiple of the critical shear stress for initiation of motion; such systems are ubiquitous in nature (Phillips and Jerolmack, 2016; Pfeiffer et al., 2017). Furthermore, bedrock rivers can behave as transport-limited systems (Johnson et al., 2009), extending the applicability of our approach. Transport-limited gravel-bed river long profiles evolve more rapidly when they are steeper and experience a greater water discharge, and more slowly when their valleys are wider, as this requires that they fill more space. We solve Equation 21 analytically for the special case in which  $dz/dt = U$  – that is, that the river neither incises nor aggrades and does not respond to tectonic or base-level forcings. Both this solution and numerical solutions of steady-state rivers with constant uplift (or subsidence) rates have a power-law form, meaning that a power law can be appropriate fit to transport-limited river long profiles.

Our derivation brings to light several significant relationships that may aid further efforts to understand river long profiles: (1) The sediment transport formula for an equilibrium-width ( $\tau_b^*/\tau_c^* = \text{constant}$ ) gravel-bed river has the stream-power form proposed by (Whipple and Tucker, 2002). We quantify the values of its coefficient and exponents. The slope exponent is  $7/6$ , and the other exponents relate to the scaling between drainage area and geomorphically effective discharge. (2) Gravel supply to rivers scales with uplift rate times contributing drainage area to a power that is less than 1, significantly modifying the implicit assumption of Whipple and Tucker (2002) that all sediment generated by rock uplift must be transported as bed load, and therefore moving the expected position of the transition between detachment- and transport-limited long profile evolution farther downstream. (3) Maintaining the observed slope–area scaling often requires that valleys widen downstream. (4) Changes in water-to-sediment discharge ratio affect channel steepness, while changes in the rate of base-level change affect channel concavity. This separation may allow the impacts of climate and tectonics to be separately inferred from channel long profiles, but increases in uplift rate are often accompanied by increases in gravel-sized sediment supply via erosional processes (e.g., landsliding) associated with increasing landscape relief. Tectonic uplift therefore can drive changes in long-profile shapes by inducing both base-level fall (reducing concavity) and an increase in sediment supply (increasing steepness). (5) The long-



observed relationship that channel width increases as the square root of discharge (Lacey, 1930; Leopold and Maddock, 1953) can be explained through a combination of valley widening and downstream fining.

In this paper, we have derived a physics-based expression for the long-profile evolution of transport-limited gravel bed rivers, whose parameters are determined by theory, experimentation, and field work. We hope that this approach to understanding gravel-bed rivers provides forward momentum towards a more formal treatment of sediment transport and fluvial morphodynamics in river long profile analysis and landscape evolution. Furthermore, by combining our derivation with other observations, we predict relationships among valley morphology, coarse sediment production and evolution, and the power-law scaling between drainage area and geomorphically effective floods. While rivers are complex, we hope that these connections with broader pieces of the geomorphic puzzle can provide a path to build a better theory of fluvial system change and landscape evolution.

*Code availability.* The GitHub repository at <https://github.com/awickert/gravel-river-long-profile> contains the “grlp” Python module, which holds functions for both the analytical and numerical solutions presented here.

## Appendix A: Notation

$z$  River bed elevation [m].

15  $t$  Time [s].

$\mathcal{S}$  Sinuosity (river length / valley length) [-].

$\lambda_p$  Porosity ( $\approx 0.65$ ) [-].

$B$  Valley width [m].

$L$  River segment length [m].

20  $Q_s$  Sediment discharge ( $=q_s b$ ) [ $\text{m}^3 \text{s}^{-1}$ ]

$x$  Downstream distance [m].

$q_s$  Sediment discharge per unit channel width [ $\text{m}^3 \text{s}^{-1}$ ].

$b$  Channel width [m].

$\phi$  Sediment transport rate coefficient ( $\approx 3.97$ ) [-]

25  $\rho_s$  Sediment density ( $\approx 2650$ ) [ $\text{kg/m}^3$ ]

$\rho$  Water density ( $\approx 1000$ ) [ $\text{kg/m}^3$ ]



- $g$  Acceleration due to gravity ( $=9.807$ ) [ $\text{m/s}^2$ ]
- $\tau_b^*$  Dimensionless bed shear stress (i.e. Shields stress) [-].
- $\tau_c^*$  Dimensionless critical shear stress (i.e. critical Shields stress) [-]
- $D$  Grain size
- 5  $\tau_b$  Bed shear stress [Pa].
- $\epsilon$  Excess bed shear stress at bankfull flow ( $\approx 0.2$ ) [-]
- $\alpha$  Angle of water surface and river bed w.r.t. horizontal [degrees or radians]
- $S$  slope of water surface and river bed ( $=\tan \alpha$ ) [-]
- $h$  Flow depth [m]
- 10  $\bar{u}$  Mean flow velocity [ $\text{m s}^{-1}$ ]
- $C_z$  Chézy coefficient (for flow velocity) [-]
- $\lambda_r$  Roughness length scale (for flow resistance) [m]
- $q$  Water discharge per unit channel width ( $=\bar{u}h$ ) [ $\text{m}^2 \text{s}^{-1}$ ]
- $Q$  Water discharge ( $=qb$ ) [ $\text{m}^3 \text{s}^{-1}$ ]
- 15  $I$  Intermittency: fraction of time at geomorphically-effective discharge [-]
- $U$  Uplift (or subsidence) rate [ $\text{m s}^{-1}$ ]
- $Q_c$  Sediment discharge capacity ( $=Q_s$  if not supply-limited) [ $\text{m}^3 \text{s}^{-1}$ ]
- $K_t$  Sediment discharge capacity power-law coefficient ( $=k_{Q_s} q_R A_R^{1-P_{AQ}}$ ) [ $\text{m}^{3-2m_t}$ ]
- $m_t$  Drainage area to sediment discharge capacity exponent ( $=P_{AQ}$ ) [ $\text{m}^3 \text{s}^{-1}$ ]
- 20  $n_t$  Slope to sediment discharge capacity exponent ( $=7/6$ ) [ $\text{m}^3 \text{s}^{-1}$ ]
- $q_R$  Rainfall flux [ $\text{m s}^{-1}$ ]
- $A_R$  Rainstorm footprint area [ $\text{m s}^{-1}$ ]
- $k_s$  Channel steepness index (slope–area coefficient) [ $\text{m}^{2\theta}$ ]
- $\theta$  Channel concavity index (slope–area space) [-]



- $\Delta$  Alluvial response rate [ $\text{m s}^{-1}$ ]
- $k_{q_s}$  Specific sediment discharge coefficient ( $\approx 0.0157$ ) [-]
- $k_b$  Threshold river width coefficient ( $\approx 2.61$ ) [-]
- $k_{Q_s}$  Sediment discharge coefficient ( $= k_{q_s} k_b \approx 0.041$ ) [-]
- 5  $A$  Drainage area [ $\text{m}^2$ ]
- $k_{AQ}$  Coefficient to relate drainage area to water discharge [ $\text{m}^{3-2P_{AQ}} \text{s}^{-1}$ ]
- $P_{AQ}$  Power to relate drainage area to water discharge [-]
- $k_{xA}$  Coefficient to relate distance downstream to drainage area [ $\text{m}^{P_{xA}-1}$ ]
- $P_{xA}$  Power to relate distance downstream to drainage area (Hack exponent) [-]
- 10  $k_{xQ}$  Coefficient to relate distance downstream to water discharge [ $\text{m}^{3-P_{xQ}} \text{s}^{-1}$ ]
- $P_{xQ}$  Power to relate distance downstream to water discharge [-]
- $k_{xB}$  Coefficient to relate distance downstream to valley width [ $\text{m}^{1-P_{xB}}$ ]
- $P_{xB}$  Power to relate distance downstream to valley width [-]
- $\beta$  Gravel production coefficient [ $\text{m}^{3-2P_\beta} \text{s}^{-1}$ ]
- 15  $P_\beta$  Gravel attenuation (weathering/fining) exponent [-]
- $P_{DQ}$  Power to relate bed-material grain size to water discharge [-]
- $z_0$  Bed elevation at  $x_0$  [m]
- $z_1$  Bed elevation at  $x_1$  [m]
- $x_0$  First (or only) known downstream distance for analytical solution [m]
- 20  $x_1$  Second known downstream distance for analytical solution [m]
- $S_0$  Upstream slope boundary condition; sets sediment input [-]
- $Q_{s_0}$  Upstream boundary condition sediment input [ $\text{m}^3 \text{s}^{-1}$ ]
- $Q_{s_{in}}$  Combined sediment input from all tributaries [ $\text{m}^3 \text{s}^{-1}$ ]



## Appendix B: Numerical solutions

### B1 Threshold-shear-stress river

Equation 21 has the form of a nonlinear advection–diffusion equation that can be rewritten for a numerical implementation as:

$$\frac{\partial z}{\partial t} = \frac{k_{Q_s} S I}{1 - \lambda_p} \left| \frac{dz}{dx} \right|^{1/6} \left[ \frac{7}{6} \frac{|Q|}{B} \frac{\partial^2 z}{\partial x^2} + \frac{1}{B} \frac{\partial |Q|}{\partial x} \frac{\partial z}{\partial x} - \frac{|Q|}{B^2} \frac{\partial B}{\partial x} \frac{\partial z}{\partial x} \right] + U \quad (\text{B1})$$

- 5 For arbitrary  $Q - x$  relationships and valley cross-sectional geometries ( $B(z(x, t))$ ), and for solutions in which the valley geometry or discharge change with time ( $B(z(x, t), t)$ ), a numerical solution becomes necessary. The above form of Equation 21 can be solved semi-implicitly as:

$$z_{i,l} = - \frac{\Delta t}{4(\Delta x)^2} \frac{k_{Q_s} S I}{1 - \lambda_p} \left| \frac{z_{i+1,l^*} - z_{i-1,l^*}}{2\Delta x} \right|^{1/6} \left[ \frac{14}{3} \left( \frac{|Q|_{i,l} + |Q|_{i,l+1}}{B_{i,l}(z_{i,l}) + B_{i,l+1}(z_{i,l^*})} \right) (z_{i+1,l+1} - 2z_{i,l+1} + z_{i-1,l+1}) + \left( \frac{(|Q|_{i+1,l} + |Q|_{i+1,l+1}) - (|Q|_{i-1,l} + |Q|_{i-1,l+1})}{B_{i,l}(z_{i,l}) + B_{i,l+1}(z_{i,l^*})} \right) (z_{i+1,l+1} - z_{i-1,l+1}) - \frac{(B_{i+1,l}(z_{i+1,l}) + B_{i+1,l+1}(z_{i+1,l^*})) - (B_{i-1,l}(z_{i-1,l}) + B_{i-1,l+1}(z_{i-1,l^*}))}{(B_{i,l}(z_{i,l}) + B_{i,l+1}(z_{i,l^*}))^2} (|Q|_{i,l} + |Q|_{i,l+1}) (z_{i+1,l+1} - z_{i-1,l+1}) \right] + z_{i,l+1} - U \Delta t \quad (\text{B2})$$

- 10 Here,  $i$  is the  $x$  index,  $l$  is the  $t$  index, and  $\Delta x$  and  $\Delta t$  are the spatial step and time step, respectively, assuming a uniform grid in space. The subscript  $l^*$  of  $z$  indicates that this term will be part of a Picard iteration: that is, it starts at  $l$  and approaches  $l + 1$  as multiple iterations of the solution provide sequentially better estimates of  $z_{l+1}$ .

Time-averaged values of  $B$  and  $Q$  are chosen to approximate conditions during the solution to the given time-step. Each of these can be simplified if  $Q$  is known (as it typically is) or varies gradually in  $t$  and/or  $B$  varies gradually in both  $z$  and  $t$ .

- 15 Using notation that they are constant in time:

$$z_{i,l} = - \frac{\Delta t}{4(\Delta x)^2} \frac{k_{Q_s} S I}{1 - \lambda_p} \left| \frac{z_{i+1,l^*} - z_{i-1,l^*}}{2\Delta x} \right|^{1/6} \left[ \frac{14}{3} \left( \frac{|Q|_i}{B_i} \right) (z_{i+1,l+1} - 2z_{i,l+1} + z_{i-1,l+1}) + \frac{|Q|_{i+1} - |Q|_{i-1}}{B_i} (z_{i+1,l+1} - z_{i-1,l+1}) - \frac{B_{i+1} - B_{i-1}}{B_i^2} |Q|_i (z_{i+1,l+1} - z_{i-1,l+1}) \right] + z_{i,l+1} - U \Delta t \quad (\text{B3})$$



This may be further simplified by moving one of the  $(1/B_i)$  terms outside of the square brackets.

For an implicit solution, the terms inside the square brackets, plus  $z_{i,l+1}$ , constitute the stencil. The slope to the  $1/6$  power term outside of the stencil is a weak nonlinearity, and nonlinearities may also be introduced by changes in  $B$  with  $z$  and/or  $t$ . The uplift term modifies a Dirichlet boundary condition at the downstream end, and is analogous with base-level rise and/or fall.

A Neumann boundary condition of sediment discharge input is used to set the slope at the upstream boundary using a “ghost-point” approach. This is solved for a defined  $Q_s$  by rearranging Equation 19 to:

$$S_0 = \text{sgn}(Q) \left( \frac{1}{k_{Q_s} I} \left| \frac{Q_s}{Q} \right| \right)^{6/7} \quad (\text{B4})$$

This demonstrates that slope increases with increasing sediment to water supply ratio, in agreement with the general principle of Lane’s balance (Lane, 1955). For a domain that begins at 0,

$$S_0 = - \left. \frac{dz}{dx} \right|_{x_0} \approx \frac{z_1 - z_{-1}}{2\Delta x}. \quad (\text{B5})$$

This equation can be rearranged to solve for the outside-domain elevation,  $z_{-1}$  in terms of values inside the domain, and both the stencil and the right-hand-side column vector for the tridiagonal matrix solution can be updated accordingly.

## B2 Valley-width-controlled river

15 The general discretization of Equation 29 for the long-profile evolution of a valley-width-confined transport-limited gravel-bed river is:

$$\begin{aligned} z_{i,l} = & -K_0 \Delta t \left( K_1 \left| \frac{z_{i+1,l^*} - z_{i-1,l^*}}{2\Delta x} \right|^{7/10} \frac{1}{D_i^{9/10} b_i^{3/5}} \left| \frac{Q_i^{3/5}}{b_i^{3/5}} - \tau_c^* \right| \right)^{1/2} D_i^{1/2} \\ & \left[ \left| \frac{z_{i+1,l^*} - z_{i-1,l^*}}{2\Delta x} \right|^{-3/10} \right. \\ & \left( \frac{3}{5} \frac{D_i^{1/10}}{|Q_i|^{2/5} b_i^{3/5}} \left( \frac{|Q|_{i+1} - |Q|_{i-1}}{2\Delta x} \right) \left( \frac{z_{i+1,l+1} - z_{i-1,l+1}}{2\Delta x} \right) \right) \\ & - \frac{3}{5} \frac{|Q_i|^{3/5} D_i^{1/10}}{b_i^{8/5}} \left( \frac{b_{i+1} - b_{i-1}}{2\Delta x} \right) \left( \frac{z_{i+1,l+1} - z_{i-1,l+1}}{2\Delta x} \right) \\ & + \frac{7}{10} \frac{|Q_i|^{3/5} D_i^{1/10}}{b_i^{3/5}} \left( \frac{z_{i+1,l+1} - 2z_{i,l+1} + z_{i-1,l+1}}{(\Delta x)^2} \right) \\ & - \frac{9}{10} \frac{|Q_i|^{3/5}}{D_i^{9/10} b_i^{3/5}} \left( \frac{D_{i+1} - D_{i-1}}{2\Delta x} \right) \left( \frac{z_{i+1,l+1} - z_{i-1,l+1}}{2\Delta x} \right) \Big) \\ & + \left( K_1 \left| \frac{z_{i+1,l^*} - z_{i-1,l^*}}{2\Delta x} \right|^{7/10} \frac{1}{D_i^{9/10} b_i^{3/5}} \left| \frac{Q_i^{3/5}}{b_i^{3/5}} - \tau_c^* \right| \right)^{1/2} \left( \frac{D_{i+1} - D_{i-1}}{2\Delta x} \right) \Big] \\ & + z_{i,l+1} - U \Delta t \end{aligned} \quad (\text{B6})$$



Here,  $K_0$  and  $K_1$  are constants standing in for sets of sediment-transport-related terms in Equation 29. This relationship is more nonlinear than that for the threshold-shear-stress river, above.

*Competing interests.* The authors declare that they have no conflict of interest.

*Acknowledgements.* This study was funded by in large part by the Emmy-Noether-Programme of the Deutsche Forschungsgemeinschaft (DFG) grant number SCHI 1241/1-1 awarded to T. Schildgen. Field and lab observations and discussions with Stefanie Tofelde, who revised an early version of the manuscript, helped to motivate the work. Early conversations on channel concavity with Kelin Whipple and Greg Tucker stimulated initial thoughts on the discussion.



## References

- Aguirre-Pe, J. and Fuentes, R.: Resistance to Flow in Steep Rough Streams, *Journal of Hydraulic Engineering*, 116, 1374–1387, [https://doi.org/10.1061/\(ASCE\)0733-9429\(1990\)116:11\(1374\)](https://doi.org/10.1061/(ASCE)0733-9429(1990)116:11(1374)), 1990.
- Aron, G. and Miller, A.: Adaptation of Flood Peaks and Design Hydrographs from Gaged to Nearby Ungaged Watersheds, *Journal of the American Water Resources Association*, 14, 313–321, <https://doi.org/10.1111/j.1752-1688.1978.tb02169.x>, 1978.
- Ashmore, P.: Channel Morphology and Bed Load Pulses in Braided, Gravel-Bed Streams, *Geografiska Annaler. Series A, Physical Geography*, 73, 37, <https://doi.org/10.2307/521212>, 1991.
- Attal, M. and Lavé, J.: Pebble abrasion during fluvial transport: Experimental results and implications for the evolution of the sediment load along rivers, *Journal of Geophysical Research: Earth Surface*, 114, 1–22, <https://doi.org/10.1029/2009JF001328>, 2009.
- 10 Attal, M., Mudd, S. M., Hurst, M. D., Weinman, B., Yoo, K., and Naylor, M.: Impact of change in erosion rate and landscape steepness on hillslope and fluvial sediments grain size in the Feather River basin (Sierra Nevada, California), *Earth Surface Dynamics*, 3, 201–222, <https://doi.org/10.5194/esurf-3-201-2015>, 2015.
- Beard, D. C. and Weyl, P. K.: Influence of Texture on Porosity and Permeability of Unconsolidated Sand, *AAPG Bulletin*, 57, 349–369, <https://doi.org/10.1306/819A4272-16C5-11D7-8645000102C1865D>, 1973.
- 15 Birnir, B., Smith, T. R., and Merchant, G. E.: The scaling of fluvial landscapes, *Computers and Geosciences*, 27, 1189–1216, [https://doi.org/10.1016/S0098-3004\(01\)00022-X](https://doi.org/10.1016/S0098-3004(01)00022-X), 2001.
- Blom, A., Viparelli, E., and Chavarrías, V.: The graded alluvial river: Profile concavity and downstream fining, *Geophysical Research Letters*, 43, 6285–6293, <https://doi.org/10.1002/2016GL068898>, 2016.
- Blom, A., Arkesteijn, L., Chavarrías, V., and Viparelli, E.: The equilibrium alluvial river under variable flow and its channel-forming discharge, *Journal of Geophysical Research: Earth Surface*, 122, 1924–1948, <https://doi.org/10.1002/2017JF004213>, 2017.
- 20 Bolla Pittaluga, M., Luchi, R., and Seminara, G.: On the equilibrium profile of river beds, *Journal of Geophysical Research: Earth Surface*, 119, 317–332, <https://doi.org/10.1002/2013JF002806>, 2014.
- Bradley, D. N. and Tucker, G. E.: Measuring gravel transport and dispersion in a mountain river using passive radio tracers, *Earth Surface Processes and Landforms*, 37, 1034–1045, <https://doi.org/10.1002/esp.3223>, 2012.
- 25 Brasington, J., Rumsby, B. T., and McVey, R. A.: Monitoring and modelling morphological change in a braided gravel-bed river using high resolution GPS-based survey, *Earth Surface Processes and Landforms*, 25, 973–990, [https://doi.org/10.1002/1096-9837\(200008\)25:9<973::AID-ESP111>3.0.CO;2-Y](https://doi.org/10.1002/1096-9837(200008)25:9<973::AID-ESP111>3.0.CO;2-Y), 2000.
- Brasington, J., Langham, J., and Rumsby, B.: Methodological sensitivity of morphometric estimates of coarse fluvial sediment transport, *Geomorphology*, 53, 299–316, [https://doi.org/10.1016/S0169-555X\(02\)00320-3](https://doi.org/10.1016/S0169-555X(02)00320-3), 2003.
- 30 Carretier, S., Regard, V., Vassallo, R., Aguilar, G., Martinod, J., Riquelme, R., Christophoul, F., Charrier, R., Gayer, E., Farías, M., Audin, L., and Lagane, C.: Differences in <sup>10</sup>Be concentrations between river sand, gravel and pebbles along the western side of the central Andes, *Quaternary Geochronology*, 27, 33–51, <https://doi.org/10.1016/j.quageo.2014.12.002>, 2015.
- Chatanantavet, P. and Parker, G.: Physically based modeling of bedrock incision by abrasion, plucking, and macroabrasion, *Journal of Geophysical Research*, 114, F04 018, <https://doi.org/10.1029/2008JF001044>, 2009.
- 35 Church, M.: Bed Material Transport and the Morphology of Alluvial River Channels, *Annual Review of Earth and Planetary Sciences*, 34, 325–354, <https://doi.org/10.1146/annurev.earth.33.092203.122721>, 2006.



- Clifford, N. J., Robert, A., and Richards, K. S.: Estimation of flow resistance in gravel-bedded rivers: A physical explanation of the multiplier of roughness length, *Earth Surface Processes and Landforms*, 17, 111–126, <https://doi.org/10.1002/esp.3290170202>, 1992.
- Costa, J. and O'Connor, J.: Geomorphically effective floods, *Geophysical Monograph Series*, 89, 45–56, 1995.
- Dingle, E. H., Attal, M., and Sinclair, H. D.: Abrasion-set limits on Himalayan gravel flux, *Nature*, 544, 471–474,  
5 <https://doi.org/10.1038/nature22039>, 2017.
- Dubinski, I. M. and Wohl, E.: Relationships between block quarrying, bed shear stress, and stream power: A physical model of block quarrying of a jointed bedrock channel, *Geomorphology*, 180–181, 66–81, <https://doi.org/10.1016/j.geomorph.2012.09.007>, 2013.
- Duvall, A.: Tectonic and lithologic controls on bedrock channel profiles and processes in coastal California, *Journal of Geophysical Research*, 109, F03002, <https://doi.org/10.1029/2003JF000086>, 2004.
- 10 Eke, E., Parker, G., and Shimizu, Y.: Numerical modeling of erosional and depositional bank processes in migrating river bends with self-formed width: Morphodynamics of bar push and bank pull, *Journal of Geophysical Research: Earth Surface*, 119, 1455–1483, <https://doi.org/10.1002/2013JF003020>, 2014.
- Fathel, S. L., Furbish, D. J., and Schmeeckle, M. W.: Experimental evidence of statistical ensemble behavior in bed load sediment transport, *Journal of Geophysical Research: Earth Surface*, 120, 2298–2317, <https://doi.org/10.1002/2015JF003552>, 2015.
- 15 Faulkner, D. J., Larson, P. H., Jol, H. M., Running, G. L., Loope, H. M., and Goble, R. J.: Autogenic incision and terrace formation resulting from abrupt late-glacial base-level fall, lower Chippewa River, Wisconsin, USA, *Geomorphology*, <https://doi.org/10.1016/j.geomorph.2016.04.016>, 2016.
- Furbish, D. J., Haff, P. K., Roseberry, J. C., and Schmeeckle, M. W.: A probabilistic description of the bed load sediment flux: 1. Theory, *Journal of Geophysical Research: Earth Surface*, 117, <https://doi.org/10.1029/2012JF002352>, 2012.
- 20 Gasparini, N. M. and Brandon, M. T.: A generalized power law approximation for fluvial incision of bedrock channels, *Journal of Geophysical Research*, 116, 1–16, <https://doi.org/10.1029/2009JF001655>, 2011.
- Gasparini, N. M., Bras, R. L., and Whipple, K. X.: Numerical modeling of non-steady river profile evolution using a sediment-flux-dependent incision model, *Geological Society of America Special Paper*, 398, 127–141, [https://doi.org/10.1130/2006.2398\(08\)](https://doi.org/10.1130/2006.2398(08)), 2006.
- Gasparini, N. M., Whipple, K. X., and Bras, R. L.: Predictions of steady state and transient landscape morphology using sediment-flux-dependent river incision models, *Journal of Geophysical Research: Earth Surface*, 112, 1–20, <https://doi.org/10.1029/2006JF000567>,  
25 2007.
- Gilbert, G. K.: Report on the Geology of the Henry Mountains, United States Government Printing Office, Washington, D.C., 1877.
- Gomez, B. and Church, M.: An assessment of bed load sediment transport formulae for gravel bed rivers, *Water Resources Research*, 25, 1161–1186, <https://doi.org/10.1029/WR025i006p01161>, 1989.
- 30 Gomez, B., Rosser, B. J., Peacock, D. H., Murray Hicks, D., and Palmer, J. A.: Downstream fining in a rapidly aggrading gravel bed river, *Water Resources Research*, 37, 1813–1823, <https://doi.org/10.1029/2001WR900007>, 2001.
- Gray, D. M.: Interrelationships of watershed characteristics, *Journal of Geophysical Research*, 66, 1215–1223, <https://doi.org/10.1029/JZ066i004p01215>, 1961.
- Hack, J.: Studies of longitudinal stream profiles in Virginia and Maryland, U.S. Government Printing Office, Washington, DC, 1957.
- 35 Harel, M. A., Mudd, S. M., and Attal, M.: Global analysis of the stream power law parameters based on worldwide  $^{10}\text{Be}$  denudation rates, *Geomorphology*, 268, 184–196, <https://doi.org/10.1016/j.geomorph.2016.05.035>, 2016.
- Hey, R. D. and Thorne, C. R.: Stable Channels with Mobile Gravel Beds, *Journal of Hydraulic Engineering*, 112, 671–689, [https://doi.org/10.1061/\(ASCE\)0733-9429\(1986\)112:8\(671\)](https://doi.org/10.1061/(ASCE)0733-9429(1986)112:8(671)), 1986.



- Hilley, G. E. and Strecker, M. R.: Processes of oscillatory basin filling and excavation in a tectonically active orogen: Quebrada del Toro Basin, NW Argentina, *Bulletin of the Geological Society of America*, 117, 887–901, <https://doi.org/10.1130/B25602.1>, 2005.
- Hobley, D. E., Sinclair, H. D., Mudd, S. M., and Cowie, P. A.: Field calibration of sediment flux dependent river incision, *Journal of Geophysical Research: Earth Surface*, 116, 1–18, <https://doi.org/10.1029/2010JF001935>, 2011.
- 5 Howard, A. D.: Thresholds in river regimes, 1980.
- Howard, A. D. and Kerby, G.: Channel changes in badlands, *Geological Society of America Bulletin*, 94, 739, [https://doi.org/10.1130/0016-7606\(1983\)94<739:CCIB>2.0.CO;2](https://doi.org/10.1130/0016-7606(1983)94<739:CCIB>2.0.CO;2), 1983.
- Ikeda, S., Parker, G., and Kimura, Y.: Stable width and depth of straight gravel rivers with heterogeneous bed materials, *Water Resources Research*, 24, 713–722, <https://doi.org/10.1029/WR024i005p00713>, 1988.
- 10 Johnson, J. P. and Whipple, K. X.: Feedbacks between erosion and sediment transport in experimental bedrock channels, *Earth Surface Processes and Landforms*, 32, 1048–1062, <https://doi.org/10.1002/esp.1471>, 2007.
- Johnson, J. P. L., Whipple, K. X., Sklar, L. S., and Hanks, T. C.: Transport slopes, sediment cover, and bedrock channel incision in the Henry Mountains, Utah, *Journal of Geophysical Research*, 114, F02014, <https://doi.org/10.1029/2007JF000862>, 2009.
- Keulegan, G. H.: Laws of turbulent flow in open channels, *Journal of Research of the National Bureau of Standards*, 21, 707, <https://doi.org/10.6028/jres.021.039>, 1938.
- 15 Komar, P. D.: Selective Grain Entrainment by a Current from a Bed of Mixed Sizes: A Reanalysis, *Journal of Sedimentary Petrology*, 57, 203–211, <https://doi.org/10.1306/212F8AE4-2B24-11D7-8648000102C1865D>, 1987.
- Komar, P. D. and Shih, S.-M.: Equal mobility versus changing bedload grain sizes in gravel-bed streams, in: *Dynamics of gravel-bed rivers*, edited by Billi, P., Hey, R. D., Thorne, C. R., and Tacconi, P., pp. 73–93, John Wiley & Sons, Chichester, United Kingdom, 1992.
- 20 Lacey, G.: Stable Channels in Alluvium, *Minutes of the Proceedings of the Institution of Civil Engineers*, 229, 259–292, <https://doi.org/10.1680/imotp.1930.15592>, 1930.
- Lamb, M. P., Dietrich, W. E., and Venditti, J. G.: Is the critical shields stress for incipient sediment motion dependent on channel-bed slope?, *Journal of Geophysical Research: Earth Surface*, 113, 1–20, <https://doi.org/10.1029/2007JF000831>, 2008.
- Lane, E. W.: Progress report on studies on the design of stable channels by the Bureau of Reclamation, *Proceedings of the American Society of Civil Engineers*, 79, 1–30, 1953.
- 25 Lane, E. W.: The Importance of Fluvial Morphology in Hydraulic Engineering, *Proceedings of the American Society of Civil Engineers*, 81, 1–17, 1955.
- Leopold, L. B. and Maddock, T.: The hydraulic geometry of stream channels and some physiographic implications, *Professional Paper*, United States Geological Survey, Washington, D.C., 1953.
- 30 Liébault, F. and Piégay, H.: Assessment of channel changes due to long term bedload supply decrease, Roubion River, France, *Geomorphology*, 36, 167–186, [https://doi.org/10.1016/S0169-555X\(00\)00044-1](https://doi.org/10.1016/S0169-555X(00)00044-1), 2001.
- Limerinos, J. T.: Determination of the Manning Coefficient From Measured Bed Roughness in Natural Channels, *USGS Water-Supply Paper* 1898-B, p. 53, 1970.
- Maritan, A., Rinaldo, A., Rigon, R., Giacometti, A., Rodriguez-Iturbe, I., and Rodríguez-Iturbe, I.: Scaling laws for river networks, *Physical Review E*, 53, 1510–1515, <https://doi.org/10.1103/PhysRevE.53.1510>, 1996.
- 35 Meyer-Peter, E. and Müller, R.: Formulas for bed-load transport, in: *Proceedings of the 2nd Meeting of the International Association for Hydraulic Structures Research*, pp. 39–64, 1948.



- Millar, R. G.: Theoretical regime equations for mobile gravel-bed rivers with stable banks, *Geomorphology*, 64, 207–220, <https://doi.org/10.1016/j.geomorph.2004.07.001>, 2005.
- Milly, P. C. D. and Eagleson, P. S.: Effect of storm scale on surface runoff volume, *Water Resources Research*, 24, 620–624, <https://doi.org/10.1029/WR024i004p00620>, 1988.
- 5 Moglen, G. E. and Bras, R. L.: The importance of spatially heterogeneous erosivity and the cumulative area distribution within a basin evolution model, *Geomorphology*, 12, 173–185, [https://doi.org/10.1016/0169-555X\(95\)00003-N](https://doi.org/10.1016/0169-555X(95)00003-N), 1995.
- Murphy, B. P., Johnson, J. P. L., Gasparini, N. M., and Sklar, L. S.: Chemical weathering as a mechanism for the climatic control of bedrock river incision, *Nature*, 532, 223–227, <https://doi.org/10.1038/nature17449>, 2016.
- Nikuradse, J.: Strömungsgesetze in Rauhen Röhren, *Forschungsheft auf dem Gebiete des Ingenieurwesens*, 361, 361, 1933.
- 10 O'Connor, J. E. and Costa, J. E.: Spatial distribution of the largest rainfall-runoff floods from basins between 2.6 and 26,000 km<sup>2</sup> in the United States and Puerto Rico, *Water Resources Research*, 40, n/a–n/a, <https://doi.org/10.1029/2003WR002247>, 2004.
- Paola, C. and Mohrig, D.: Palaeohydraulics revisited: palaeoslope estimation in coarse-grained braided rivers, *Basin Research*, 8, 243–254, <https://doi.org/10.1046/j.1365-2117.1996.00253.x>, 1996.
- 15 Paola, C., Heller, P. L., and Angevine, C. L.: The large-scale dynamics of grain-size variation in alluvial basins. I: Theory, *Basin Research*, 4, 73–90, <https://doi.org/10.1111/j.1365-2117.1992.tb00145.x>, 1992.
- Parker, G.: Self-formed straight rivers with equilibrium banks and mobile bed. Part 2. The gravel river, *Journal of Fluid Mechanics*, 89, 127, <https://doi.org/10.1017/S0022112078002505>, 1978.
- Parker, G.: Downstream variation of grain size in gravel rivers: Abrasion versus selective sorting, in: *Fluvial Hydraulics of Mountain Regions*, edited by Armanini, A. and Di Silvio, G., vol. 37 of *Lecture Notes in Earth Sciences*, pp. 345–360, Springer, Berlin, Heidelberg, <https://doi.org/10.1007/BFb0011201>, 1991.
- 20 Parker, G., Klingeman, P. C., and McLean, D. G.: Bedload and size distribution in paved gravel-bed streams, *Journal of the Hydraulics Division*, 108, 544–571, 1982.
- Parker, G., Paola, C., Whipple, K. X., and Mohrig, D.: Alluvial Fans Formed by Channelized Fluvial and Sheet Flow. I: Theory, *Journal of Hydraulic Engineering*, 124, 985–995, [https://doi.org/10.1061/\(ASCE\)0733-9429\(1998\)124:10\(985\)](https://doi.org/10.1061/(ASCE)0733-9429(1998)124:10(985)), 1998.
- Pfeiffer, A. M., Finnegan, N. J., and Willenbring, J. K.: Sediment supply controls equilibrium channel geometry in gravel rivers, *Proceedings of the National Academy of Sciences*, 114, 201612907, <https://doi.org/10.1073/pnas.1612907114>, 2017.
- Phillips, C. B. and Jerolmack, D. J.: Self-organization of river channels as a critical filter on climate signals, *Science*, 352, 694–697, <https://doi.org/10.1126/science.aad3348>, 2016.
- 30 Pitlick, J., Mueller, E. R., and Segura, C.: Relation between flow, surface-layer armoring and sediment transport in gravel-bed rivers, *Earth Surface Processes and Landforms*, 33, 1192–1209, <https://doi.org/10.1002/esp>, 2008.
- Roering, J. J., Kirchner, J. W., and Dietrich, W. E.: Evidence for nonlinear, diffusive sediment transport on hillslopes and implications for landscape morphology, *Water Resources Research*, 35, 853–870, <https://doi.org/10.1029/1998WR900090>, 1999.
- Savenije, H. H.: The width of a bankfull channel; Lacey's formula explained, *Journal of Hydrology*, 276, 176–183, [https://doi.org/10.1016/S0022-1694\(03\)00069-6](https://doi.org/10.1016/S0022-1694(03)00069-6), 2003.
- 35 Savi, S., Schildgen, T. F., Tofelde, S., Wittmann, H., Scherler, D., Mey, J., Alonso, R. N., and Strecker, M. R.: Climatic controls on debris-flow activity and sediment aggradation: The Del Medio fan, NW Argentina, *Journal of Geophysical Research: Earth Surface*, 121, 2424–2445, <https://doi.org/10.1002/2016JF003912>, 2016.



- Schildgen, T. F., Robinson, R. A. J., Savi, S., Phillips, W. M., Spencer, J. Q. G., Bookhagen, B., Scherler, D., Tofelde, S., Alonso, R. N., Kubik, P. W., Binnie, S. A., and Strecker, M. R.: Landscape response to late Pleistocene climate change in NW Argentina: Sediment flux modulated by basin geometry and connectivity, *Journal of Geophysical Research: Earth Surface*, 121, 392–414, <https://doi.org/10.1002/2015JF003607>, 2016.
- 5 Shields, A.: Anwendung der Aehnlichkeitsmechanik und der Turbulenzforschung auf die Geschiebebewegung, Doktor-ingenieurs dissertation, Technischen Hochschule Berlin, Berlin, 1936.
- Shobe, C. M., Tucker, G. E., and Anderson, R. S.: Hillslope-derived blocks retard river incision, *Geophysical Research Letters*, 43, 5070–5078, <https://doi.org/10.1002/2016GL069262>, 2016.
- Simpson, G. and Castelltort, S.: Model shows that rivers transmit high-frequency climate cycles to the sedimentary record, *Geology*, 40, 1131–1134, <https://doi.org/10.1130/G33451.1>, 2012.
- Singh, V. P.: On the theories of hydraulic geometry, *International Journal of Sediment Research*, 18, 196–218, 2003.
- Sklar, L. and Dietrich, W. E.: River longitudinal profiles and bedrock incision models: Stream power and the influence of sediment supply, in: *Rivers Over Rock: Fluvial Processes in Bedrock Channels*, edited by Tinkler, K. J. and Wohl, E. E., vol. 107 of *Geophysical Monograph Series*, pp. 237–260, American Geophysical Union, Washington, D.C., <https://doi.org/10.1029/GM107p0237>, 1998.
- 15 Sklar, L. S. and Dietrich, W. E.: Sediment and rock strength controls on river incision into bedrock, *Geology*, 29, 1087–1090, 2001.
- Sklar, L. S. and Dietrich, W. E.: A mechanistic model for river incision into bedrock by saltating bed load, *Water Resources Research*, 40, 1–22, <https://doi.org/10.1029/2003WR002496>, 2004.
- Sklar, L. S., Riebe, C. S., Marshall, J. A., Genetti, J., Leclere, S., Lukens, C. L., and Mercedes, V.: The problem of predicting the size distribution of sediment supplied by hillslopes to rivers, *Geomorphology*, 277, 31–49, <https://doi.org/10.1016/j.geomorph.2016.05.005>, 2017.
- 20 Slack, J. R. and Landwehr, J. M.: Hydro-climatic data network (HCDN); a U.S. Geological Survey streamflow data set for the United States for the study of climate variations, 1874–1988, U.S. Geological Survey, Menlo Park, CA, 1992.
- Snow, R. S. and Slingerland, R. L.: Mathematical Modeling of Graded River Profiles, *The Journal of Geology*, 95, 15–33, <https://doi.org/10.1086/629104>, 1987.
- Snyder, N. P., Whipple, K. X., Tucker, G. E., and Merritts, D. J.: Stream profiles in the Mendocino triple junction region, northern California, *GSA Bulletin*, 112, 1250–1263, [https://doi.org/10.1130/0016-7606\(2000\)112<1250:lrrtfd>2.3.co;2](https://doi.org/10.1130/0016-7606(2000)112<1250:lrrtfd>2.3.co;2), 2000.
- 25 Sólyom, P. B. and Tucker, G. E.: Effect of limited storm duration on landscape evolution, drainage basin geometry, and hydrograph shapes, *Journal of Geophysical Research*, 109, F03 012, <https://doi.org/10.1029/2003JF000032>, 2004.
- Sternberg, H.: Untersuchungen über längen- und querprofil geschiebeführender Flüsse, *Zeitschrift für Bauwesen*, 25, 483–506, 1875.
- Strahler, A. N.: Quantitative Geomorphology of drainage basin and channel Networks, in: *Handbook of Applied Hydrology*, edited by Chow, V. T., pp. 4–76, McGraw–Hill, New York, New York, USA, 1964.
- 30 Sullivan, T. U. F. S. and Lucas, W. U. F. S.: Chronic Misapplication of the Relationship between Magnitude and Frequency in Geomorphic Processes, As Illustrated in *Fluvial Processes in Geomorphology* by Leopold, Wolman and Miller (1964), *Advancing the Fundamental Sciences: Proceedings of the Forest Service National Earth Sciences Conference*, pp. 4–6, 2007.
- Tomkin, J. H., Brandon, M. T., Pazzaglia, F. J., Barbour, J. R., and Willett, S. D.: Quantitative testing of bedrock incision models for the Clearwater River, NW Washington State, *Journal of Geophysical Research: Solid Earth*, 108, <https://doi.org/10.1029/2001JB000862>, 2003.
- Tucker, G. E. and Slingerland, R.: Drainage basin responses to climate change, *Water Resources Research*, 33, 2031–2047, <https://doi.org/10.1029/97wr00409>, 1997.



- Whipple, K. K. X.: Fluvial landscape response time: How plausible is steady-state denudation?, *American Journal of Science*, 301, 313–325, <https://doi.org/10.2475/ajs.301.4-5.313>, 2001.
- Whipple, K. X.: Bedrock Rivers and the Geomorphology of Active Orogens, *Annual Review of Earth and Planetary Sciences*, 32, 151–185, <https://doi.org/10.1146/annurev.earth.32.101802.120356>, 2004.
- 5 Whipple, K. X. and Tucker, G. E.: Dynamics of the stream-power river incision model: Implications for height limits of mountain ranges, landscape response timescales, and research needs, *Journal of Geophysical Research: Solid Earth*, 104, 17 661–17 674, <https://doi.org/10.1029/1999JB900120>, 1999.
- Whipple, K. X. and Tucker, G. E.: Implications of sediment-flux-dependent river incision models for landscape evolution, *Journal of Geophysical Research*, 107, 10.1029/2000JB000 044, 2002.
- 10 Whipple, K. X., Hancock, G. S., and Anderson, R. S.: River incision into bedrock: Mechanics and relative efficacy of plucking, abrasion, and cavitation, *Geological Society of America Bulletin*, 112, 490–503, [https://doi.org/10.1130/0016-7606\(2000\)112<490:RIIBMA>2.0.CO;2](https://doi.org/10.1130/0016-7606(2000)112<490:RIIBMA>2.0.CO;2), 2000.
- Wilcock, P. R. and Crowe, J. C.: Surface-based Transport Model for Mixed-Size Sediment, *Journal of Hydraulic Engineering*, 129, 120–128, [https://doi.org/10.1061/\(ASCE\)0733-9429\(2003\)129:2\(120\)](https://doi.org/10.1061/(ASCE)0733-9429(2003)129:2(120)), 2003.
- 15 Willgoose, G., Bras, R. L., and Rodriguez-Iturbe, I.: A coupled channel network growth and hillslope evolution model: 1. Theory, *Water Resources Research*, 27, 1671–1684, <https://doi.org/10.1029/91WR00935>, 1991.
- Wolman, M. G.: A method of sampling coarse river bed material, *Transactions, American Geophysical Union*, 35, 951–956, <https://doi.org/10.1029/TR035i006p00951>, 1954.
- Wolman, M. G. and Miller, J. P.: Magnitude and frequency of forces in geomorphic processes, *Journal of Geology*, 68, 54–74, 1960.
- 20 Wong, M. and Parker, G.: Reanalysis and Correction of Bed-Load Relation of Meyer-Peter and Müller Using Their Own Database, *Journal of Hydraulic Engineering*, 132, 1159–1168, [https://doi.org/10.1061/\(ASCE\)0733-9429\(2006\)132:11\(1159\)](https://doi.org/10.1061/(ASCE)0733-9429(2006)132:11(1159)), 2006.